applied sciences

MDPI

Article

Investigating the Impact of Wildfires on Lake Water Quality Using Earth Observation Satellites

Rossana Caroni [1,*], Monica Pinardi [1], Gary Free [1], Daniela Stroppiana [1], Lorenzo Parigi [1], Giulio Tellina [1], Mariano Bresciani [1], Clément Albergel [2] and Claudia Giardino [1]

[1] CNR—Institute for Electromagnetic Sensing of the Environmental, Via A. Corti 12, 20133 Milan, Italy; pinardi.m@irea.cnr.it (M.P.); gary.free@ec.europa.eu (G.F.); stroppiana.d@irea.cnr.it (D.S.); parigi.l@irea.cnr.it (L.P.); tellina.g@irea.cnr.it (G.T.); bresciani.m@irea.cnr.it (M.B.); giardino.c@irea.cnr.it (C.G.)

[2] European Space Agency Climate Office, ECSAT, Harwell Campus, Oxfordshire, Didcot OX11 0FD, UK; clement.albergel@esa.int

* Correspondence: caroni.r@irea.cnr.it

Abstract: A study was carried out to investigate the effects of wildfires on lake water quality using a source dataset of 2024 lakes worldwide, covering different lake types and ecological settings. Satellite-derived datasets (Lakes_cci and Fire_cci) were used and a Source Pathway Receptor approach applied which was conceptually represented by fires (burned area) as a source, precipitation/drought representing transport dynamics, and lakes as the ultimate receptor. This identified 106 lakes worldwide that are likely prone to be impacted by wildfires via a terrestrial pathway. Satellite-derived chlorophyll-a (Chl-a) and turbidity variables were used as indicators to detect changes in lake water quality potentially induced by wildfires over a four-year period. The lakes with the largest catchment areas burned and characterized by regular annual fires were located in Africa. Evidence for a strong influence of wildfires was not found across the dataset examined, although clearer responses were seen for some individual lakes. However, among the hydro-morphological characteristics examined, lake depth was found to be significant in determining Chl-a concentration peaks which were higher in shallow and lower in deep lakes. Lake turbidity responses indicated a dependence on lake catchment and weather conditions. While wildfires are likely to contribute to the nutrient load of lakes as found in previous studies, it is possible that in many cases it is not a dominant pressure and that its manifestation as a signal in lake Chl-a or turbidity values depends to a large part on lake typology and catchment characteristics. Assessment of lake water quality changes six months after a fire showed that Chl-a concentrations either increased, decreased, or showed no changes in a similar number of lakes, indicating that a lake specific ecological and hydro-morphological context is important for understanding lake responses to wildfires.

Keywords: lake water quality; lake catchment; satellite remote sensing; wildfires; climate change

Citation: Caroni, R.; Pinardi, M.; Free, G.; Stroppiana, D.; Parigi, L.; Tellina, G.; Bresciani, M.; Albergel, C.; Giardino, C. Investigating the Impact of Wildfires on Lake Water Quality Using Earth Observation Satellites. *Appl. Sci.* **2024**, *14*, 2626. https://doi.org/10.3390/app14062626

Academic Editors: Tom Lotz, Christian Opp and Oleg S. Pokrovsky

Received: 2 February 2024
Revised: 16 March 2024
Accepted: 19 March 2024
Published: 21 March 2024

1. Introduction

Climate change, particularly global warming and increasing drought, is leading to an increased frequency and severity of wildfires [1]. As a consequence of global warming, heatwaves are becoming more frequent, more intense, and lasting longer [2]. When high temperatures are combined with dry vegetation and low air humidity, it increases the risk of wildfire outbreak when there is a source of ignition [3]. This combination of conditions is now observed over longer periods of time over much of the world [4].

Among the many impacts of wildfires are those on aquatic ecosystems, both via atmospheric deposition of aerosols and via terrestrial runoff within lake catchments where fires occur. Wildfires can have an impact on river and lake water quality by altering the physical, chemical, and biological characteristics of soils and aquatic ecosystems [5]. Much research has focused on the consequences of wildfires on terrestrial ecosystems and air

quality, while until recently the effects of wildfires on water quality have been relatively overlooked [6–8], while the majority of research concerning the aquatic impacts of wildfires is based on streams and rivers rather than lakes.

In this study, we investigated how wildfires might affect lakes through the terrestrial pathway, potentially mediated by weather and catchment characteristics; in particular, we used the Source-Pathway-Receptor (SPR) approach. Environmental scientists first used the SPR conceptual model in the late 1970s to describe the potential flow of contaminants from a source to potential receptors via different pathways [9]. In freshwater systems, lakes are considered receptors or sinks in which material and pollutants tend to accumulate and pathways are processes of transport, dilution, and transformation of pollutants in their catchments. The SPR model has been applied as a simple conceptual model for illustrating systems and processes leading to a specific outcome in several environmental risk assessments [10–12], such as flood risks and erosion [13–15].

The SPR approach could hence be used to also show how the transport of burned material from wildfires can follow the terrestrial pathway via lake catchment, promoted by periods of rainfall, to finally reach a receptor lake and ultimately affect its water quality. It is in fact acknowledged that wildfires can have an important impact on the geomorphology and hydrology of river catchments, particularly regarding rainfall post-wildfire events leading to runoff, soil erosion, and transport processes which could result in lake water quality changes [16,17]. These impacts are a function of time since the fire event, and depend on fire types, lake trophic status, and landscape characteristics [3]. Lake ecological context is indeed important to explain and predict lake responses to fire events, since impacts may be mediated by weather, catchment, and lake typology [5].

Studies in burned river catchments have revealed that soil erosion and increased sediment load can occur, with a magnitude depending on intensity and the frequency of post-fire rainfall and associated flow events [18–20], with increased runoff volume and velocity of transport to lakes in the catchment [21,22]. Along with the key role of flow, particularly during storm events, research from a deforested catchment where vegetation regrowth was inhibited revealed a dramatic increase in particulate export owing to increased erodibility after two years, being more than twice as important as hydrological changes. Loss of dissolved nitrogen and phosphorus also increased tenfold [23]. This may be particularly relevant given the increasing frequency of fires that may limit regrowth leading to increased erodibility of soils with important consequences for stream and lake systems. In addition, wildfires have the potential to release nutrients and organic matter stored in soils and vegetation, allowing them to be transferred to aquatic ecosystems [24]. Input of burned material is expected to increase water turbidity in lakes and to temporarily decrease water transparency. Following a fire, concentrations of phosphorus and nitrogen, the two most generally limiting nutrients for primary producers in lakes, frequently increase in aquatic systems [25,26].

Recently, some general patterns and responses of wildfire effects on water quality have emerged [27], including increased concentrations of nutrients, ions, organic material, and a general decrease in water clarity, following post-fire increments in erosion and runoff while changes in chlorophyll-a were less consistent [28]. A recent review of 44 studies worldwide [5] comparing pre- and post-fire water quality field sampling data found that wildfires increased post-fire nutrient export relative to pre-fire levels within a one-year time lag between sampling and fire occurrence. Previous research on the impact of fires on lakes was restricted in terms of lake number, geographical regions, and ecological contexts, with the majority of studies carried out on a limited number of lakes ($\leq$15). In this context, there is a need for broad scale research on a large number of lakes, covering many geographical regions and different ecological settings, in order to assess the generalizability of the findings. Remote sensing techniques can be used to achieve these objectives by producing datasets providing global, objective, and consistent information on burned areas, active fires, and water quality products. These datasets are increasingly being used to monitor the state of the Earth's systems [29,30]. Remote sensing data could help fill

the knowledge gap on the long- and short-term effects of wildfires on lake water quality, complementing traditional field sampling data.

The aim of this study was to investigate the potential impacts of wildfires on lake water quality at a global scale. To this end, we used satellite products developed by two separate projects on lakes (Lakes_cci) and fire (Fire_cci) managed by the European Space Agency Climate Change Initiative (ESA CCI). The dataset included 2024 lakes allowing for the investigation of a large number of lakes distributed globally and covering a wide range of hydro-morphological and ecological settings combined with burned area data from Fire_cci (FireCCI51; [31]) for a time period of about 20 years. In particular, we aimed at testing whether changes in the satellite-derived chlorophyll-a (Chl-a) concentration and turbidity represented signals of lake water response to fire disturbance, both in terms of the magnitude of peaks and development time following a sequence of fire and precipitation events in their catchments. The SPR approach was adopted because our investigation focused on the effects of wildfires on lakes via the terrestrial pathway, and the approach provided a framework to select lakes whose waters were likely to be most affected by wildfires, given their catchment characteristics and precipitation conditions. A final subset of 106 lakes distributed globally was investigated to evaluate the impact of fire disturbance on lake water quality, through interpreting changes in the satellite products of Chl-a and turbidity.

2. Materials and Methods

2.1. Datasets

In this study, from the different variables from the Lakes_cci project [32], we considered Chl-a and turbidity as indicators of water quality for the period from 2017 to 2020 built from OLCI-Sentinel-3 A/B data. In addition, both the Lake Ice Cover (LIC) and Lake Surface Water Temperature (LSWT) variables were considered; the first to focus our analysis on ice-cover free periods, the second as an ancillary observation to evaluate water quality changes. We used the FireCCI51 Burned Area (BA) product, which shows the global spatio-temporal distribution of BA derived from MODIS satellite observations [31]. Burned area maps are produced using a hybrid algorithm that blends active fire derived from thermal channels with the highest resolution near-infrared (NIR) surface reflectance (~250 m) [33]. The product comprises monthly global maps covering the period 2001–2020 and burned pixels are recorded with the estimated Julian day (DOY) of detection and the land cover category of the burned pixels, extracted from the Land Cover_cci v2.0.7 product [34]. Burned pixels have been extracted from the FireCCI51 BA product for every catchment connected to any of the lakes included in the Lakes_cci database for the considered period. The extraction was performed using the R package "exactextractr" [34], allowing for the retrieval of the exact coverage fraction of a pixel on the basin polygons.

Lake and catchment area data were obtained from the HydroLAKES and HydroBASINS datasets. The HydroLAKES database [35] was used to obtain the following attribute information for the 2024 lakes investigated: lake surface area (km^2), length of shoreline (km), shoreline development (ratio shoreline length/circumference of a circle with the same area), total lake volume (million cubic meters), mean water depth (m), mean long-term discharge flowing through a lake ($m^3\ s^{-1}$), mean water residence time (days), elevation of lake surface (m a.s.l.), lake latitude and longitude, area of the catchment associated with the lake (km^2). Every lake is co-registered to a sub-catchment of the HydroBASINS database (via shared IDs). We obtained the hydrologic areas of the 2024 lakes from the HydroBASINS database [36] which provides vectorized polygon layers that show sub-basin boundaries at a global scale. Using the HydroBASINS dataset, sub-basins connected to each lake have been selected. The database allows us to navigate sub-basins upstream from the lake, and all the sub-basins connected within 50 steps (levels 0–50) from a lake have been assigned accordingly with this approach; the presence of a lake in the connection chain causes the interruption of the navigation. The basins within four steps (levels 0–4) represent the

nearest to the lake basin, and are thus considered the closest catchment areas around a lake in our analysis.

Land cover data at lake catchment level was extracted from the Copernicus Climate Change Service [37] for the period 2017–2020.

We calculated the Standardized Precipitation Index (SPI; [38]) for each lake for the period 1980–2019 using ERA5 data of total precipitation for each lake watershed (sum of hourly values to obtain daily data) with the reference period set to 1980–2010. The SPI is a statistical indicator that compares the total (median) precipitation falling at a given location during a given period (12 months for this work) with the distribution of long-term precipitation for the same period. Negative index values identify moderately to extremely dry conditions, while positive values identify very to moderately wet conditions; values in the range [−1, 1] identify close to normal conditions with respect to the long-term trend. The Standardized Precipitation Index (SPI) mean, minimum, and maximum were calculated for each year and for the whole considered period (2017–2020).

2.2. Data and Statistical Analysis

According to the SPR approach adopted in this study [9,10], which describes the transport of burned materials to lakes through terrestrial pathways, from the initial 2024 lakes of the Lakes_cci dataset, an initial selection of lakes to be considered in our data analysis was performed. To achieve this, similar types of wildfires were identified and grouped together based on the type of land cover type burned and on the frequency of fires. Hierarchical cluster analysis was performed using Sørensen distance with flexible beta linkage. The resulting dendrograms were grouped according to the minimization of the indicator (p-value = 0.010) [39].

Our data analysis focused on the period 2017–2020 since during the last decade wildfire occurrence has escalated, and also for data consistency as satellite-derived Chl-a and turbidity products of the selected timeframe derive from the same optical sensor (OLCI onboard Sentinel-3 A/B).

A classification of lake trophic status was carried out on the basis of mean Chl-a concentration, calculated for the period 2017–2020, according to OECD (1982): oligotrophic < 2.5 mg m^{-3}; mesotrophic from 2.5 to 8 mg m^{-3}; eutrophic from 8 to 25 mg m^{-3}; hypertrophic > 25 mg m^{-3}.

Satellite-derived BA data were used to calculate the ratio of burned area/burnable area (sum of burned area and unburned area) (BA/A) for each lake investigated; in particular, in our investigation we considered the ratio for the maximum area burned in the whole lake catchment (0–50 levels identified with the HydroBASINS dataset) and the ratio for the closest catchment area burned around a lake, identified in the first four steps (level 0–4) calculated for each lake for each year.

An Analysis of Variance (ANOVA or Kruskal–Wallis) test and box plots were used to investigate Chl-a and turbidity concentration differences between depth groups (shallow (<7 m), medium (7–15 m), and deep (>15 m) lakes, according to [40]), as well as trophic status (oligotrophic, mesotrophic, eutrophic, hypertrophic) and burned land cover vegetation.

A Stepwise Multiple Linear Regression (SMLR; [41]) was performed to investigate the most likely factors that explain maximum annual Chl-a and turbidity peaks among the variables: lake surface area, length of shoreline, shoreline development, lake volume, mean water depth, mean long-term discharge, mean water residence time, elevation, latitude and longitude, catchment area, ratio catchment area/lake area, mean SPI for the period (2017–2020), SPI mean per year, mean BA/A ratio (2017–2020), maximum BA/A ratio per year, BA/A level 0–4 per year, total precipitation, normalized difference between max Chl-a peak and mean Chl-a per year, and normalized difference between max turbidity peak and mean turbidity per year.

The concentration of Chl-a and turbidity peaks following a fire event was calculated using the "zoo" R package [42]. A lowess line (a locally weighted non-parametric smoothing method) was fitted to the dataset with a data span of 10% and a window half-width of 5 days, allowing for the identification of local maxima; missing daily values were linearly

interpolated, which should not change the maximum value recorded, but may reduce the accuracy of the result.

The average satellite observation frequency for the dataset over the study period was 1.7 days, which is close to the recommended sampling frequency of once every two days required to detect short-term perturbations in phytoplankton dynamics [43] and compares favorably with large-scale in situ synoptic sampling efforts. It is also well above the frequencies recommended by EU policy [44–46]. The timing of Chl-a and turbidity peaks after a fire occurrence were also identified by this analysis.

Boosted regression analysis was carried out to analyze factors (lake area, shore length and development, total lake volume, lake average depth, water residence time, lake elevation, watershed area, longitude, latitude, ratio catchment area/lake area, mean ratio BA/A, ratio BA/A level 0–4, ratio total BA/A, maximum BA, annual SPI mean, min, and max, total annual rainfall) determining the timing of the first peak and maximum peak of Chl-a and turbidity after a fire [47]. Analysis was carried out on 75% of the data with 25% used for model evaluation by calculating the Root Mean Square Error (RMSE). Analysis was carried out in R package 'gbm' [48].

To determine short-term effects of fire on lake Chl-a and turbidity, we compared mean concentrations over a six-month period after a maximum fire occurrence with mean concentrations over a six-month period either without or with smaller fires using R (package dplyr [49]). Multinomial logistic regression with "nnet" R package [50] was performed in order to investigate the role of geographical factors (i.e., altitude, latitude), land cover types, maximum fire, and total annual rainfall in determining changes in water quality (i.e., Chl-a and turbidity).

Finally, lake responses to typological factors and in-lake interactions were analyzed using a graphical analysis [51] which allows for a comparison of the timeseries data of different parameters: fire occurrence and intensity (BA), an indicator of precipitation/drought (SPI), lake surface water temperature (LSWT), and lake water quality parameters such as Chl-a concentration (smoothed) and turbidity concentration (smoothed). These timeseries graphs allow for the investigation of the temporal succession of events in a lake catchment and the identification of lake case studies to support statistical analysis results.

3. Results

3.1. Selection of Lakes by SPR Approach

A hierarchical cluster analysis (Sørensen distance) was performed using the FireCCI product to identify and group comparable types of wildfires based on the land cover type burned. Based on the minimization of the indicator *p*-value (=0.010), the resulting dendrogram was divided into six groups. These groups showed that half of the clusters, i.e., clusters 1, 2, and 3, represented a total of 1578 lakes (78% of the 2024 lakes in the dataset) and had few records of burned areas, while the remaining clusters 4, 5, and 6 were characterized by the more consistent occurrence of wildfires (446 lakes, or 22% of the dataset). Regarding the vegetation types and the regions identified as subject to burning, Cluster 4 consisted of burned evergreen coniferous forestry in North America and Canada, Cluster 5 featured crops or natural shrubbery in America, Eurasia, and Australia, and Cluster 6 was more diversified and included the most burned areas of deciduous broad leaves, which are common in the southern hemisphere, especially in Africa (Table 1 clusters 1–6 in rows). Figure 1 shows the map of the six vegetation clusters.

To support this analysis, a second cluster analysis on the total burned area for an extended period (2001–2020) was performed identifying five end groups. Two clusters, cluster I and II, contained 1394 lakes (69% of the total lakes) that had few records of burned areas, while the remaining clusters II, IV, and V were characterized by a higher frequency of wildfires and larger burned areas (630 lakes, 31%) (Table 1, clusters I–V in columns). In particular, Cluster IV was characterized by hydrological areas where a high proportion was burned every year, frequently more than 3–4% of the catchment area, and similarly Cluster III identified hydrological basins with frequent fires (annual) but only in 0.1–0.2% of the

catchment area, while Cluster V had limited fire peaks and burned areas. We derived a contingency matrix by joining the results of the two clustering analysis, thereby identifying agreement on lakes where major wildfires occurred for the different land cover types (bold numbers in Table 1). From this table, we selected these candidate lakes covering a range of different land cover types and with different fire regimes (fire frequency and intensity), excluding lakes in catchments with small (low BA) and rare fires. As a result, a total of 314 lakes were therefore selected for further investigation.

Table 1. Contingency matrix of 2024 lakes selected via clustering of land cover burned (2011) and total area burned (2001–2020). Potential geographical and land cover combinations with burn temporal pattern (frequency/intensity). Number of lakes included in the selected clusters are highlighted in bold (n = 314).

Vegetation Type and Distribution		**Rare Fires and Low BA**	**Rare Fires and Very Low BA**	**Limited Regular Annual Fires and Medium BA**	**Significant Regular Annual Fires and High BA**	**Limited Fire Peaks and Medium BA**	***Total***
	Cluster	I	II	III	IV	V	
Needleleaf deciduous (Global)	1	383	698	128	15	57	*1281*
Needleleaf, evergreen (Northern temperate)	2	43	48	14	0	40	*145*
Crops/Herbaceous (Global)	3	71	19	53	6	3	*152*
Boreal forest (Canada)	4	54	10	**13**	0	**18**	*95*
Crops—natural shrubbery (Eurasia)	5	51	0	**114**	**13**	**2**	*180*
Deciduous broad leaves (Africa, India, South America)	6	17	0	**93**	**61**	0	*171*
	Total	*619*	*775*	*415*	*95*	*120*	*2024*

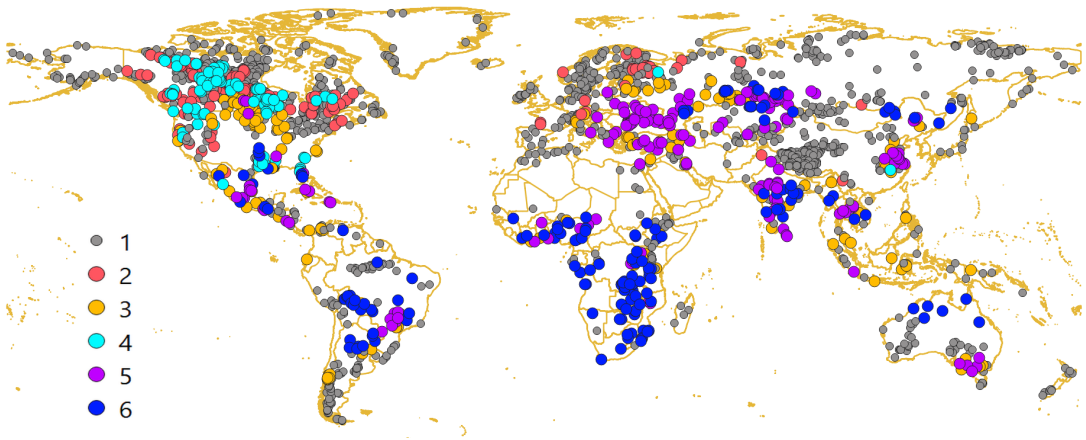

Figure 1. Global map of the six vegetation clusters burned in 2011. Land cover indicator values of each cluster are reported in Table S1.

Because we are focusing on the terrestrial pathway of burned materials transported to lakes, the previous analysis on vegetation and fire intensity and frequency provides an indication of changes in hydrological pathways as a result of vegetation loss. Catchments that experience significantly seasonal or variable rainfall leading to overland flow may be

among the most vulnerable [52]. We used as a proxy for precipitation the SPI calculated for the period 1980–2019. Positive SPI values identify moderately to very wet conditions in the catchment. The other factor considered was the catchment to lake area ratio, with low values indicating lakes potentially having a long residence time while high values would typically have a short residence time and be more strongly influenced by their drainage area.

The ratio catchment area/lake area was calculated and plotted against the SPI for the 314 lakes selected from the previous cluster analysis (contingency matrix in Table 1), allowing the identification of lakes that were potentially more prone to pollution (burned materials and released nutrients) from wildfire occurrence in their catchments (Figure 2). In particular, lakes having a 95th percentile of SPI > 1.5 and a catchment area to lake area ratio > 30 (close to the limit identified by other authors [53–55] located in the upper right part of the plot in Figure 2) have been identified as lakes more influenced by catchment dynamics and terrestrial transport. These lakes should thus potentially be more prone to be receptors of fire-derived substances and would eventually have more affected water quality. These criteria used in lake selection identified a total of 153 lakes selected for further consideration in our analysis.

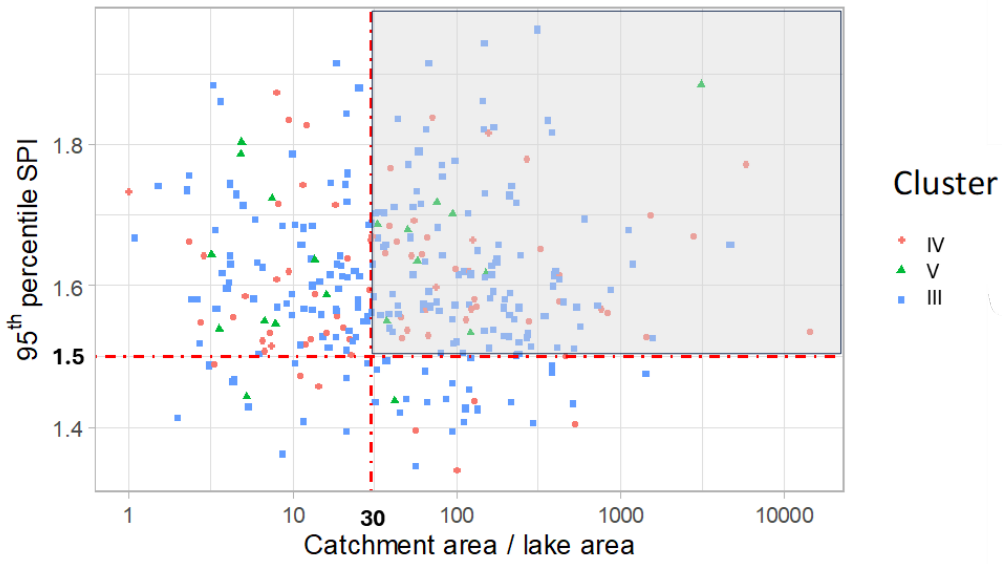

Figure 2. Lakes from contingency matrix (Table 1) plotted as a function of the catchment area/lake area ratio (horizontal-axis) and the 95th percentile of SPI (vertical-axis). Lakes in the upper right quarter (95th percentile SPI > 1.5 and catchment area/lake area ratio > 30) for cluster III (limited regular annual burning), cluster IV (significant regular annual burning), and cluster V (limited burning peaks) were selected for further investigation (n = 153).

The method of data extraction utilized five regions of interest (ROI) within the Lakes_cci product layers for Chl-a and turbidity and was applied for the subset of the 153 lakes to ensure lake pixels had a 96% presence of water. Following these criteria, 47 lakes were excluded from the analysis, leaving a final number of 106 lakes with reliable data to be analyzed. The final list of the 106 lakes selected is presented in Table S2 in the Supplementary Materials.

3.2. Lake Characteristics

The 106 lakes finally selected for analysis represented a significant latitudinal and altitude gradient (30° S to 60° N; −2 to 1518 m a.s.l.) across multiple ecoregions (from Boreal to Tropical). The lakes cover a wide range of hydro-morphological characteristics for mean depth, lake surface area, and diverse trophic levels (by Chl-a concentration) (Table 2). According to the OECD trophic classification, 1 lake was oligotrophic, 29 were mesotrophic,

58 were eutrophic, and 18 were hypereutrophic (Figure S1A in the Supplementary Materials). Based on the Lake_cci turbidity products for the period 2017–2020, we found that most of the lakes (69%) had mean turbidity between 1.5 and 5 NTU, 14% < 1.5 NTU, 13% between 5 and 10 NTU, 7% in the range 10–20 NTU, and the remaining 3% up to 40 NTU (Figure S1B in the Supplementary Materials).

Table 2. Water quality and hydro-morphological characteristics of the selected 106 lakes.

	Mean Chl-a 2017–2020 (mg m^{-3})	Mean Turbidity 2017–2020 (NTU)	Lake Area (km^2)	Total Volume (km^3)	Mean Depth (m)	Residence Time (Days)	Elevation (m a.s.l.)
Mean	18.6	4.6	1005	23,691	13.9	536	318
Min	1.7	0.6	15	34	0.1	0.2	−2
Max	146.9	39.0	26,734	1,580,000	59.2	11,794	1518

Out of a total of 106 lakes, 41 lakes were identified as shallow (mean depth < 7 m), 31 as medium depth (mean depth between 7 and 15 m), and the remaining 34 as deep (mean depth > 15 m). A total of 43% of lakes have a surface < 250 km^2, 41% between 250 and 1000 km^2, 10% up to 3000 km^2, and the remaining six largest lakes reach an area up to a maximum value of 26,734 km^2 (Great Slave Lake, Canada) (Figure S1C in the Supplementary Materials). Lake volume for 25% of the lakes was < 500 km^3, 25% between 500 and 3000 km^3, 28% between 3000 and 10,000 km^3, 21% up to 150,000 km^3, and Great Slave Lake has the maximum value with 1,580,000 km^3 (Figure S1D in the Supplementary Materials). For lake water residence time, 30 lakes had a fast renewal < 2 months, 46 lakes between 2 and 12 months, 15 lakes up to 2 years, 13 lakes had a slower residence time from 4 up to 33 years (Figure S1E in the Supplementary Materials). Finally, our dataset has 17% of lakes at an altitude < 50 m a.s.l., 74% between 50 and 700 m a.s.l., and 9% up to 1800 m a.s.l. (Figure S1F in Supplementary Materials).

For these 106 lakes, the corresponding BA/A ratios for the period 2017–2020 were distributed as follows: six lakes (located in Africa) had a mean annual ratio BA/A > 0.40, eight lakes had ratios between 0.40 and 0.25, and the remaining lakes had a ratio < 0.25 (Figure 3).

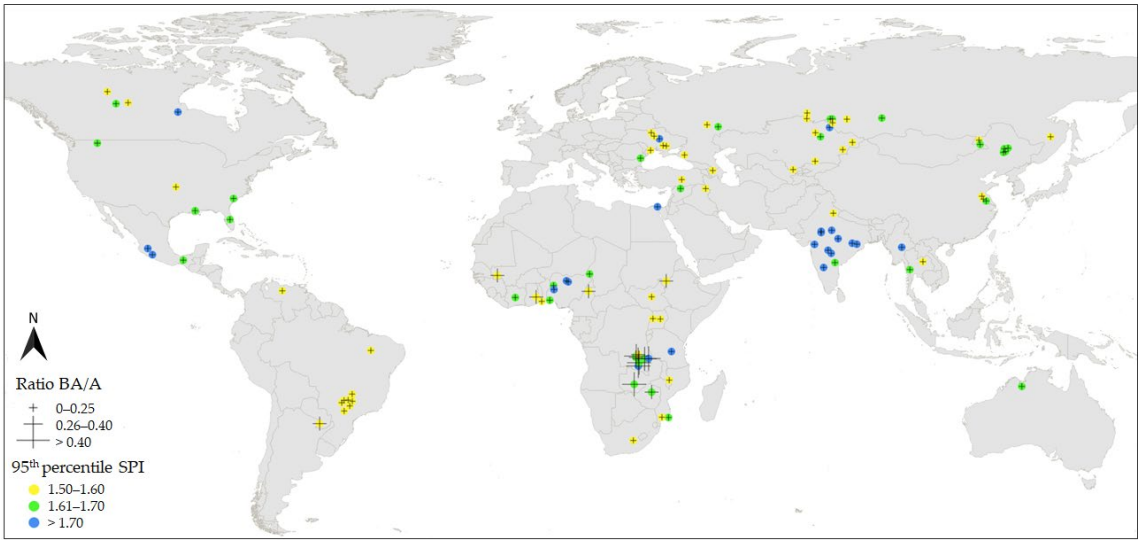

Figure 3. Map with geographical location of the 106 lakes selected. Ratio burned area/burnable area (BA/A) and the 95th percentile of the Standardized Precipitation Index (SPI) are reported.

3.3. Determination of Peaks in Chl-a and Turbidity Concentrations

Among all lake hydro-morphological parameters considered (listed in the Section 2) we found that mean depth was a significant factor to group lakes according to water quality responses to wildfire occurrence. In the 106 lakes analyzed, Chl-a concentration (both as annual mean concentration and maximum peak concentration) was greater in shallow lakes than in medium and deep lakes (Figure 4). We found that maximum peak concentrations of Chl-a were significantly higher in shallow lakes (median = 24.8 mg m^{-3}; N = 164;) than in medium depth lakes (19.9 mg m^{-3}; N = 124) and deep lakes (median = 12.2 mg m^{-3}; N = 136) ($p < 0.001$; Figure 4b) (where N represents the number of lakes for each year analyzed from 2017 to 2020).

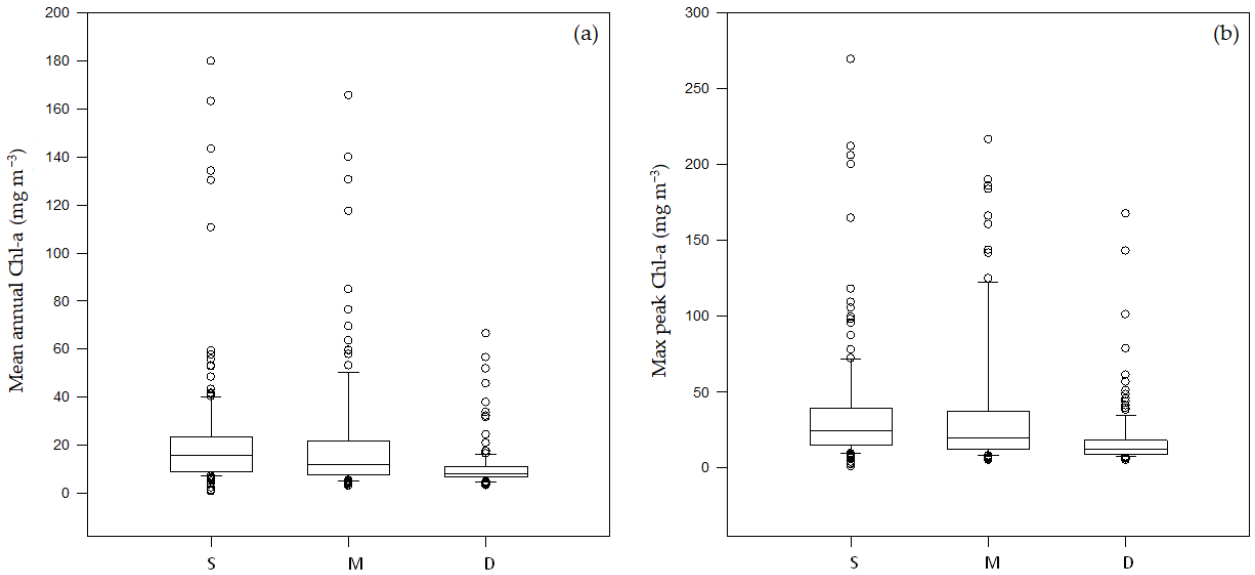

Figure 4. Chlorophyll-a mean annual concentration (**a**) and maximum peak concentration (**b**) in lakes separated into three groups according to lake mean depth. S = shallow (<7 m), M = medium (7–15 m), D = deep (>15 m).

A Stepwise Multiple Linear Regression (SMLR) was performed in order to investigate factors that were significant in determining maximum annual Chl-a and turbidity peaks in the selected lakes (Table 3). These factors included lake geo-morphological characteristics, burned areas, the ratio BA/A calculated in the whole catchment and in the closest part of a lake (level 0–4), and SPI variation. The SMLR results confirmed that lake depth (−; $p < 0.001$) was the most significant factor to predict maximum Chl-a peaks, followed by lake latitude (+; $p < 0.001$). Mean values of BA/A (+) and mean SPI (−) improved the regression to a final R^2 = 19.5%. Multiple linear regression analysis to predict maximum turbidity peaks revealed mean SPI as a significant parameter (+; $p < 0.05$), but explained a very small amount of variation (1.2%), with no additional significant variables in the analysis.

Table 3. Results of Stepwise Multiple Regression Analysis results for chlorophyll-a (Chl-a) and turbidity maximum peak concentrations as dependent variables. Left column = all lakes. Right column = lakes having a significant regular annual burning, located mainly in the African continent.

Chl-a Peak (Log)	**R^2 = 19.5%**		**Chl-a Peak (Log) (Cluster IV)**	**R^2 = 45.8%**	
Variable	**Coefficient**	***p***	**Variable**	**Coefficient**	***p***
Depth_mean	−0.0067	0.0001	Depth_mean	−0.4107	0.0001
Latitude	0.0046	0.0001	Residence time (Log)	0.2341	0.0001
BA/A_mean	0.2652	0.0218	BA level 0–4 (Log)	−0.1310	0.0001
SPI_mean	−0.0676	0.0057	SPI (90th percentile)	0.6872	0.0279
Turbidity (NTU)	R^2 = 1.2%		**Turbidity (NTU) (Cluster IV)**	R^2 = 42.3%	
Variable	**Coefficient**	***p***	**Variable**	**Coefficient**	***p***
SPI_mean	0.5341	0.0275	Elevation	−0.0004	0.0001
			Log Catchment/lake area	0.3511	0.0001
			SPI_mean	1.9097	0.0001

We also restricted SMLR analysis to lakes having a significant regular annual burning and a high BA/A annual ratio in their catchment, located mainly in the African continent (cluster IV as reported in Table 1, N = 24; Table 3 right part). For Chl-a, SMLR performed on this restricted group of lakes confirmed that lake depth was the principal factor in predicting maximum peak concentration (−; $p < 0.001$), followed by water residence time (+; $p < 0.001$), burned area closest to the lake (level 0–4) (−; $p < 0.001$), and SPI (90th percentile) (+; $p = 0.028$), resulting in a final R^2 = 45.8%. SMLR analysis for predicting turbidity maximum peaks, performed in the same restricted lakes group, resulted in lake elevation (−; $p < 0.001$), log ratio catchment area/lake area (+; $p < 0.001$), and mean SPI (+; $p < 0.001$) as significant factors giving a final R^2 = 42.3%.

Graphical analysis of time series data provides example lake cases to examine in more detail for our global findings. Figure 5 shows the time series for two lakes with the most extensive burned areas in their catchment (BA annual mean over 10,000 km^2), located in the Sub-Saharan belt in Africa and having a regular annual burning frequency. Lake Volta (Ghana) is a large (6045 km^2) and deep lake (average depth = 24.5 m), and Lake Chad (Chad/Niger) is very large (18,751 km^2) and very shallow (average depth = 0.1 m). The two lakes have comparable wildfire frequency and intensity, with high BA/A ratio (0.14 to 0.38) and similar SPI range. General patterns of smoothed fit of turbidity and Chl-a showed that concentrations were more stable and with moderate concentration peaks (mean peaks: turbidity = 5.6 NTU; Chl-a = 14.8 mg m^{-3}) in the deeper Lake Volta, and more variable with more pronounced peaks in the shallow Lake Chad (mean peaks: turbidity = 17.3 NTU; Chl-a = 20.7 mg m^{-3}).

Additional cases supporting the importance of lake depth can be found in three other lakes located in the South American continent, with comparable burned areas in their catchment, with similar SPI values and different lake depths, Lake Verà (Paraguay) being a shallow lake (average depth = 2.2 m), Lake Guarico (Venezuela) medium (average depth = 9.8 m), and Lake da Brisas (Brazil) deep (average depth = 51.2 m). Their Chl-a response to fire was quite diverse and more evident in the shallowest Lake Verà, which experienced a steep progressive increase after two successive important fires in 2020 (increased from 15 to over 50 mg m^{-3}, annual mean from 16 to 25 mg m^{-3} in 2020).

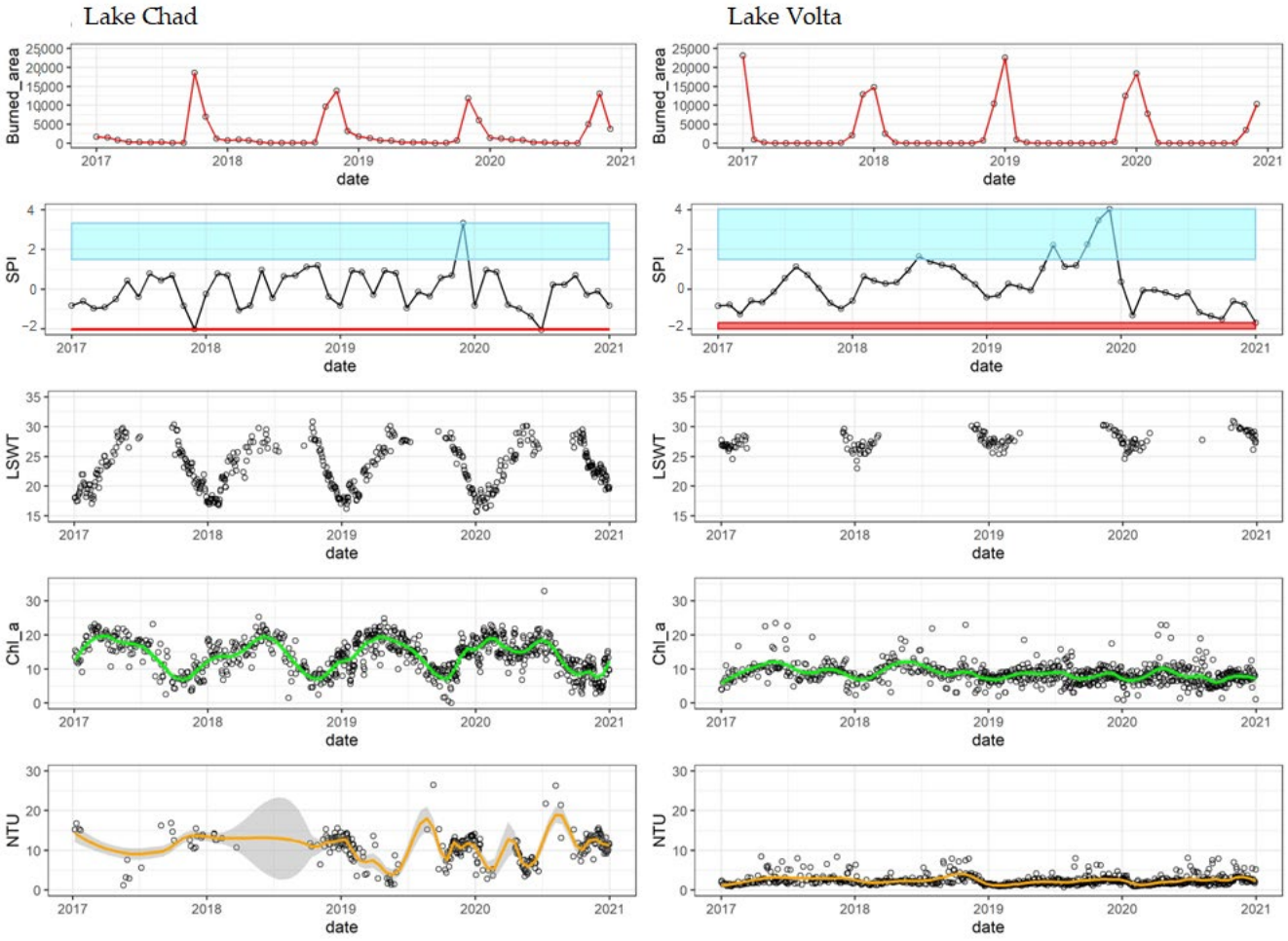

Figure 5. Time series data of burned area (km^2), standardized precipitation index (SPI; red and light blue boxes for extremely dry and wet conditions, respectively), water temperature (LSWT; T°), chlorophyll-a (Chl-a; mg m^{-3}), and turbidity (NTU) of Lake Chad (Chad/Niger) and Lake Volta (Ghana).

3.4. Time of Occurrence of Chl-a and Turbidity Peaks after a Fire

When Chl-a and turbidity peaks succeeded a fire event, we were able to calculate the time (expressed in days) and concentration (mg m^{-3}) of the peaks occurring after a fire. We calculated the first detected peak of Chl-a and turbidity occurring immediately after a fire occurrence and the maximum peak developed during the year. The median timing of the first detected post-fire Chl-a peak was 58 days (mean ± standard deviation = 65 ± 45 days) across all lakes investigated, and for the majority (58%) of lake-year cases the first peak of Chl-a appeared within 90 days from the fire event (Figure 6a). The median time of the maximum annual Chl-a peak that developed after a fire was 103 days (mean ± sd = 110 ± 72 days) across all lakes and resulted in a similar percentage of lake-year cases (7–8%) up to 150 days (Figure 6b). The median number of days for the first peak in turbidity after a fire was 68 days (mean ± sd = 72 ± 52 days) across all lakes, and for most lake-year cases (52%), the first peak of turbidity occurred within 75 days from the fire event (Figure 6a). The median time of the maximum annual peak of turbidity was 151 days (mean ± sd = 163 ± 85 days) after a fire event (Figure 6b). The two largest lakes in our dataset (Great Slave Lake in Canada and Lake Chad in Central Africa) had a relatively fast response in developing the first turbidity peak after a fire, within 70 days, and most other large lakes (lake area > 2000 km^2) had a response within four months (122 days) after a fire.

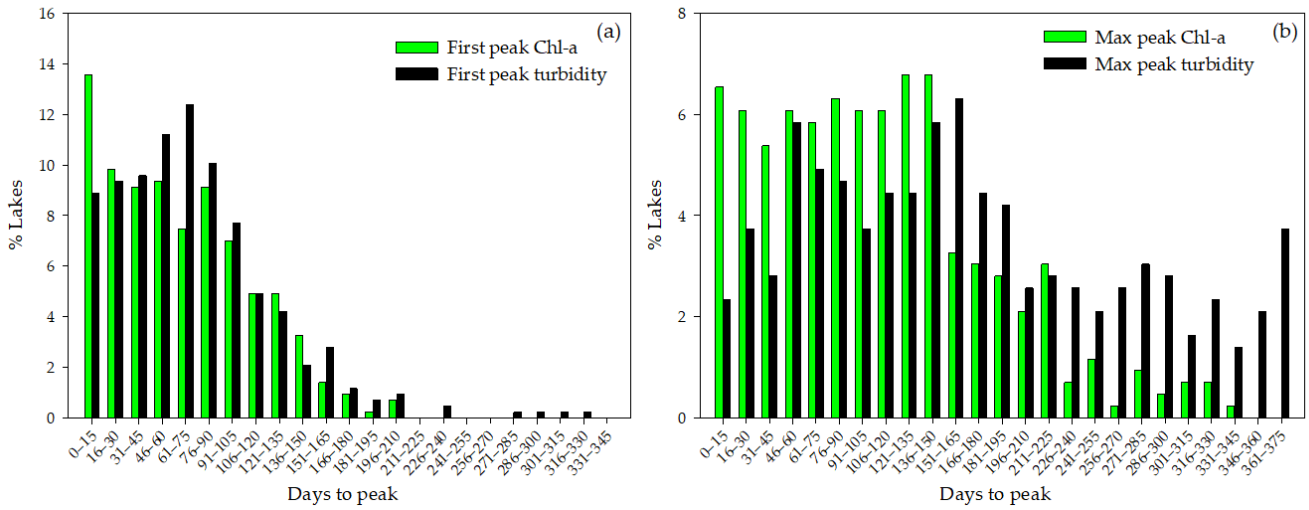

Figure 6. Frequency distribution, as percentage of lakes (annual data per each lake from 2017 to 2020), of the time interval [days] between the occurrence of a fire and the detection of the first peak (**a**) and the maximum peak (**b**) of Chl-a (green bars) and turbidity (black bars).

The analysis of timing in peak development for Chl-a and turbidity identified the successive concentration peaks after a fire's occurrence and the results were used for investigating relationships with burned areas in lake catchments. Burned area parameters were calculated and considered both as a ratio of burned area over total burnable area in the catchment (ratio BA/A) and burned area over the closest burnable area to a lake (ratio BA/A level 0–4). We found that in general, lakes with a higher proportion of burned area in relation to burnable catchment area showed a faster timing for developing maximum peaks of Chl-a (Figure 7), although the noise in the data did not allow us to fit a significant trend in the relationship. The timing for development of Chl-a maximum peaks in years when lakes had an annual BA/A level 0–4 (Figure 7a) ratio > 0.25 was 90 days on average (N = 41) and in a relatively restricted time range (153 days), while when the BA/A (level 0–4) ratio was <0.25, the mean was 112 days (N = 307) in a wider time range (339 days). For the ratio BA/A (Figure 7b), the days to the Chl-a maximum peak was on average 102 days (N = 60) with ratio > 0.25, while when the BA/A ratio was <0.25 the mean was 114 days (N = 288). Patterns of the ratio BA/A with the timing of the first peaks of Chl-a and with both the first and the maximum peaks of turbidity were less distinct.

In order to investigate further the influence of fire and precipitation parameters on the timing of peak development for Chl-a and turbidity, we ran a boosted regression analysis. Models produced by this regression were weak based on the high values of Root Mean Square Error (RMSE), which ranged from 48 to 63 days. Although the models should not be overinterpreted, the factors estimated to have the most influence for Chl-a and turbidity were SPI, maximum BA, lake position (latitude and longitude) and total rainfall. Results are shown in Figure S2 in the Supplementary Materials.

When the timing of the peaks in Chl-a and turbidity that developed after a fire was analyzed by grouping lakes according to ecological characteristics, such as lake trophic conditions, we observed that oligotrophic lakes were slightly faster (mean ± sd = 94 ± 63 days) than mesotrophic (mean ± sd = 105 ± 64 days), eutrophic (mean ± sd = 120 ± 81 days), and hypereutrophic (mean ± sd = 99 ± 81 days) lakes in developing maximum Chl-a peaks after a fire (Figure 8a). In this analysis, trophic classification was slightly adjusted to include a representative number of lake years for each trophic group (i.e., oligotrophic lakes with annual mean Chl-a < 5 mg m^{-3}). However, both first and maximum Chl-a peak concentrations were smaller in oligotrophic than in higher trophic lakes, as presented in Figure 8b showing scatterplots of the relationships between lake trophic status, expressed as Chl-a mean concentrations (over

the period 2017–2020), and Chl-a concentration of first peaks (Figure 8b) and maximum peaks (Figure 8c) developed after a fire.

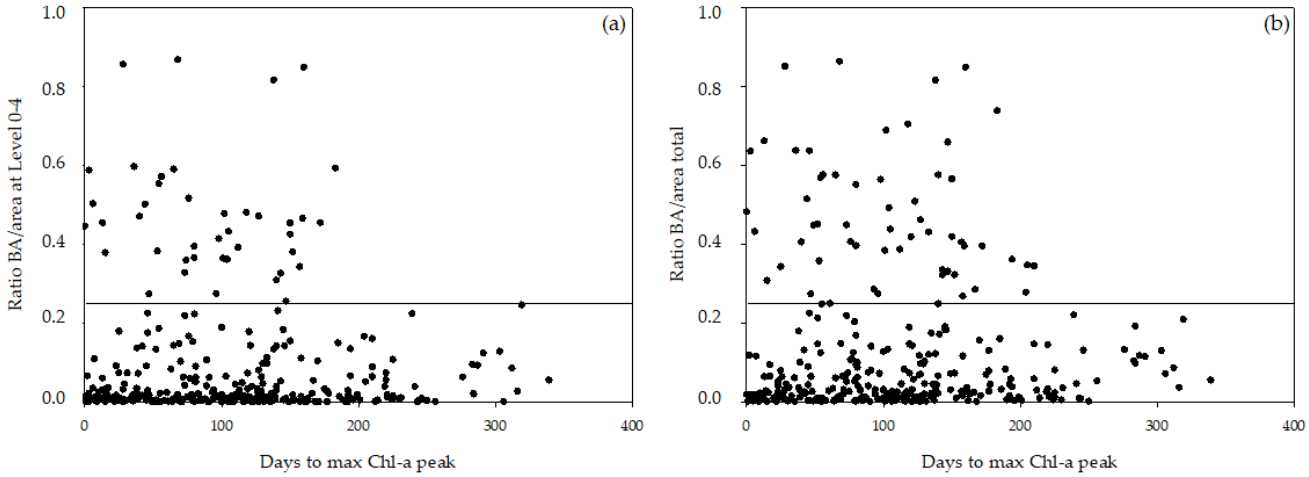

Figure 7. Scatterplot of the ratio of the burned area/burnable area at level 0–4 (BA/area at level 0–4) (**a**) and the ratio of the burned area/total burnable area in the catchment (BA/area total) (**b**) versus development time of maximum peaks of Chl-a (days) since fire occurrence in the studied lakes (lake_year). The black lines identify a ratio of 0.25.

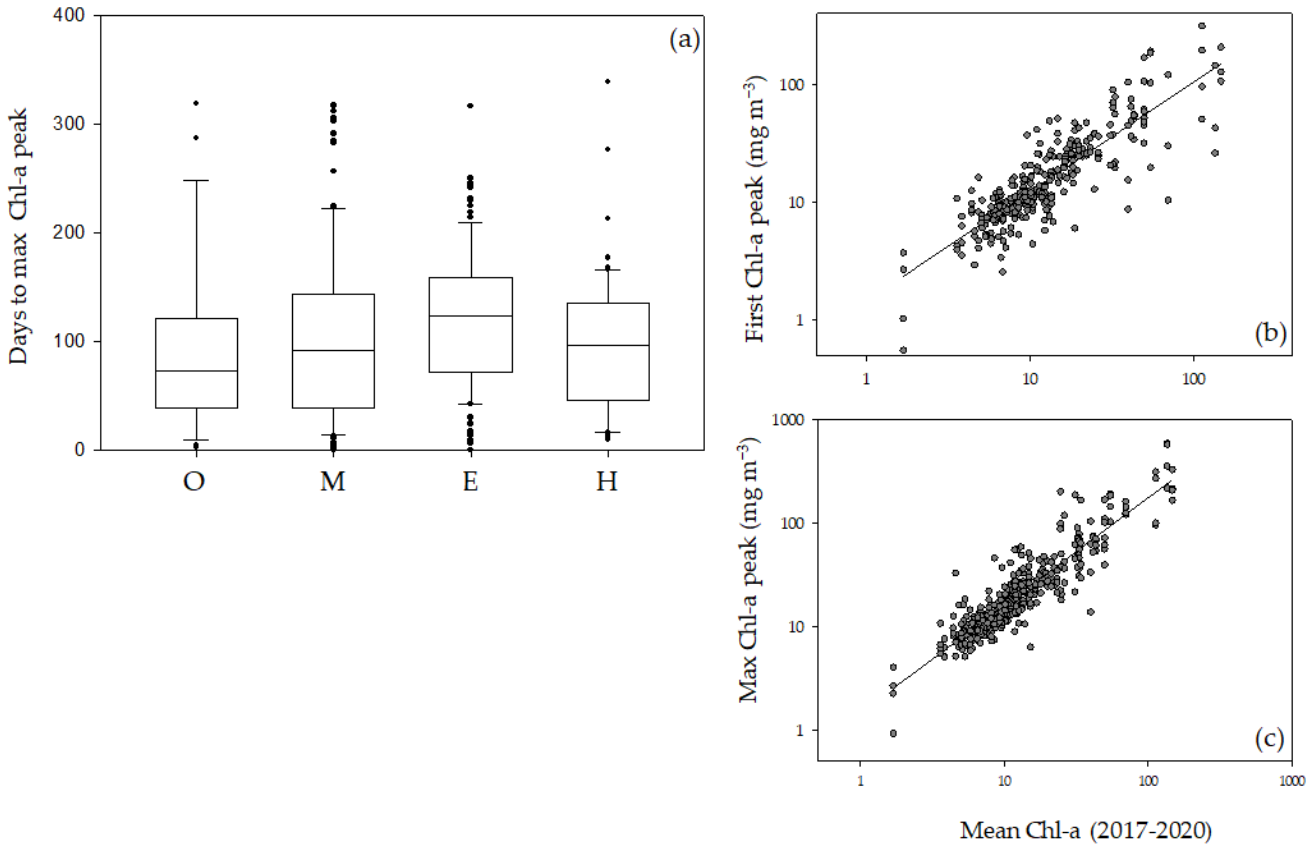

Figure 8. Boxplots of lake trophic classes (O = oligotrophic, M = mesotrophic, E = eutrophic, H = hypereutrophic) and timing (days) of max Chl-a peak development (**a**). Scatterplots between lake chlorophyll-a (Chl-a) mean concentration (2017–2020; mg m^{-3}) and Chl-a concentration of first peaks ($R^2 = 0.732$, $p < 0.001$) (**b**) and maximum peaks ($R^2 = 0.826$, $p < 0.001$) (**c**).

We also investigated whether the type of land cover burned influenced the timing of Chl-a and turbidity peaks. Using the clustering results of the burned land cover types presented in Table 1, we found a significant difference in ANOVA for Chl-a ($p = 0.002$) but not for turbidity ($p > 0.05$). A Bonferroni post-hoc test indicated that the difference was between Cluster 4 (corresponding to evergreen boreal forests) and Cluster 6 (deciduous broad leaves) ($p = 0.007$), with a mean of 63 ± 50 days for Cluster 4 and 120 ± 68 days for Cluster 6 (Figure 9). A difference in total annual precipitation (m) among these clusters was also found, being highest in Cluster 6 (mean of 0.91 ± 0.46 m), while in contrast, the annual maximum values of the SPI were found to be significantly higher in Cluster 4 (mean of 1.72 ± 0.80) (ANOVA $p = 0.002$).

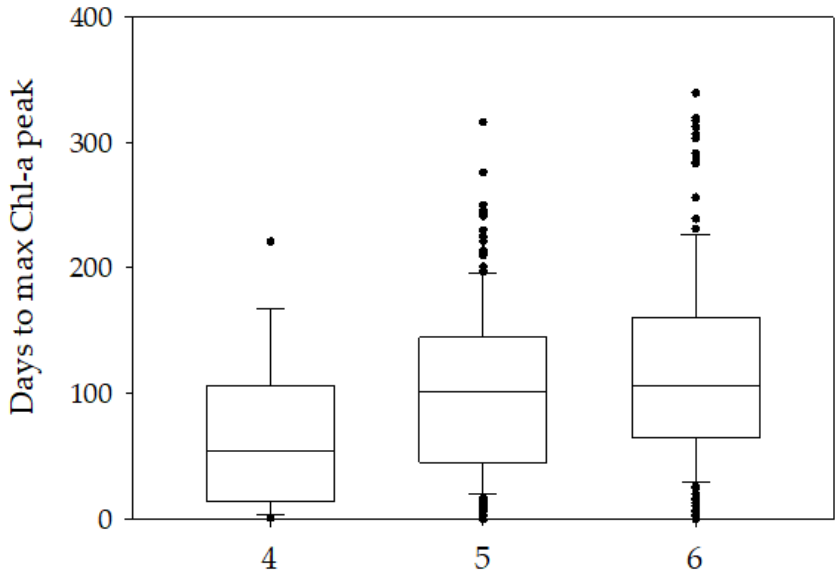

Figure 9. Boxplot of burned land cover clusters (4 = evergreen boreal forest; 5 = crops to natural shrubbery; 6 = deciduous broad leaves), and timing (days) of max Chl-a peak development.

3.5. Post-Fire Water Quality Assessment

To determine whether a change in average concentration of Chl-a and turbidity happened after a fire in the catchment of our studied lakes for the period 2017–2020, we calculated the mean Chl-a and turbidity concentrations over a six-month period after a maximum fire occurrence and compared with mean concentrations over the same six months either without or with smaller fires. From the initial number of 106 lakes, 7 lakes have been excluded from the analysis because the occurrence of their major fires was close to the end of the studied period (end of year 2020). Thus, the period following the major fire was shorter than six months, leaving a final number of 99 lakes analyzed for this assessment.

Figure 10 shows the global distribution of lakes in different classes according to positive or negative changes (in percentage) of Chl-a and turbidity. For Chl-a, 28 lakes showed an increase (>10%), 33 lakes had no relevant change (range −10 to +10%), and 38 lakes showed a decrease (>−10%) in Chl-a concentration six months after maximum fire occurrence. For turbidity, 37 lakes showed an increase, 38 lakes had no relevant change, and 24 lakes showed a decrease in turbidity concentration six months after maximum fire occurrence.

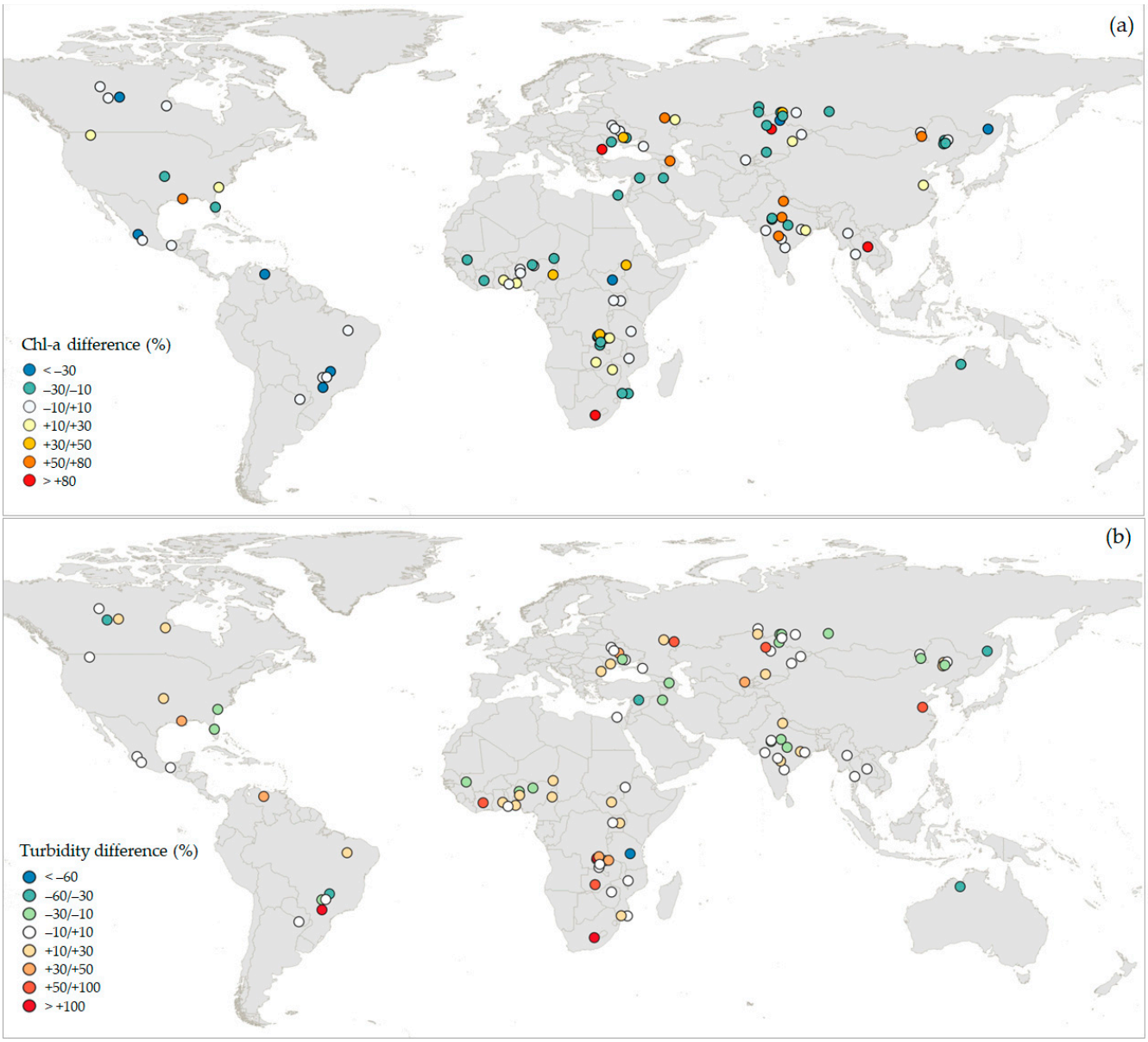

Figure 10. Global map showing geographical distribution of lakes with (**a**) chlorophyll-a (Chl-a) and (**b**) turbidity % change, calculated as the difference between mean concentration over a six-month period after maximum fire occurrence and after no or weaker/smaller fire occurrence.

There are no evident geographical patterns of increases or decreases in the concentration of parameters, except for a prevalence of a percentage increase in turbidity in African lakes (Figure 10b). Regarding lake characteristics, hypereutrophic lakes showed the most relevant positive changes (mean percentage difference in Chl-a of 29%).

In order to see which explanatory variables might influence the trends in Chl-a and turbidity, we carried out a multinomial logistic regression using the lakes grouped as stable (=no change), increasing, and decreasing. The pool of predictors was increased sequentially starting with just latitude and altitude, then landcover types were added, and finally also total annual rainfall and the maximum fire peak were included. However, none of the included parameters were found to be significant in determining the trend in either Chl-a or turbidity (Table S3 in the Supplementary Materials).

3.6. In-Lake Interactions between Chl-a and Turbidity

The time series plots showed some cases where peaks in water turbidity concentration occurred and corresponded, or might have led, to lake Chl-a concentration decreases (Figure 11). These interactions were observed in diverse lake typologies according to depth such as Lake Togo (Africa) (a shallow lake), Lake Mtera (Tanzania, Africa) (a medium lake), and Lake Hirakud (India) (a deep lake). The succession of events is particularly evident in the shallow Lake Togo where a fire occurred at the beginning of 2019 and then eight months after a period of high precipitation occurred and was followed by a peak of turbidity (above 10 NTU) and a depression of Chl-a which then increased to maximum values when turbidity stabilized to lower values (mean 3.3 NTU). In Lake Mtera, after a major fire in 2019 was followed by a precipitation period, turbidity greatly increased (above 25 NTU) while Chl-a remained suppressed for the rest of the entire period considered (from annual mean concentration of 45.1 mg m^{-3} during 2018 to 14.3 mg m^{-3} during 2020). In Lake Hirakud, a time series is clearly shown every year with a correspondence between the occurrence of turbidity peaks and Chl-a concentration decline.

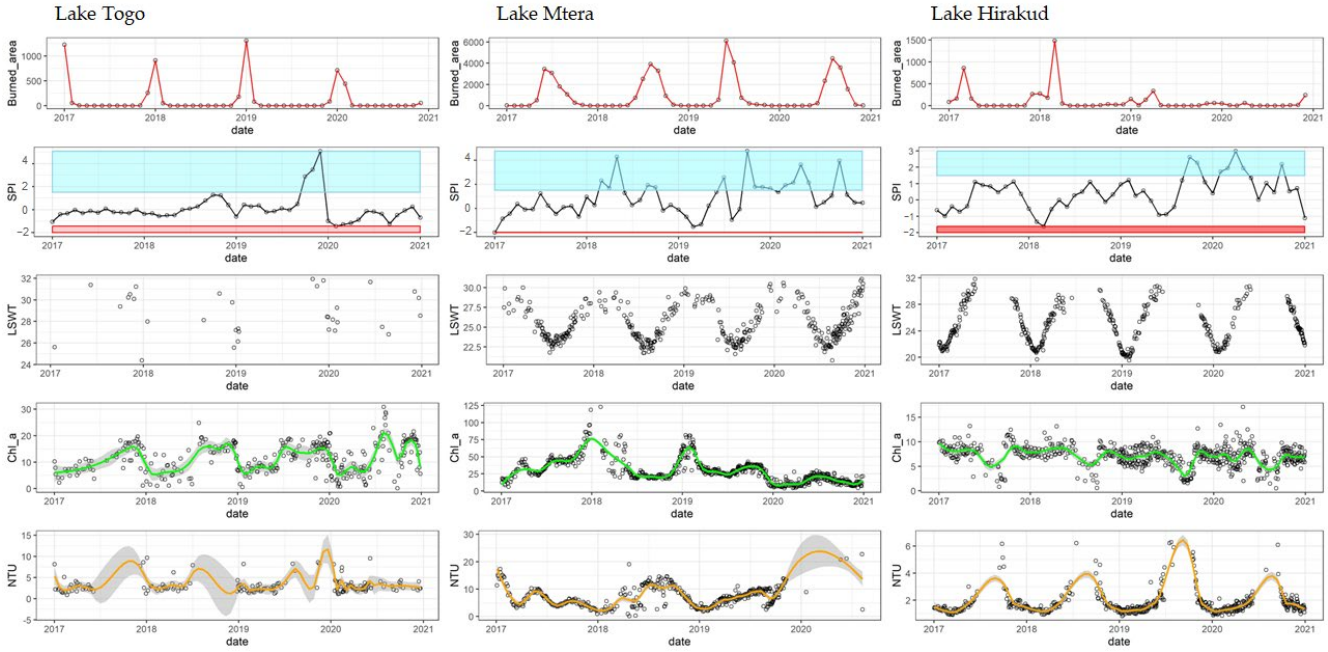

Figure 11. Time series data of burned area (km^2), standardized precipitation index (SPI; red and light blue boxes: extremely dry and wet conditions, respectively), water temperature (LSWT; C°), Chl-a (mg m^{-3}), and turbidity (NTU) in Lake Togo (Togo), Lake Mtera (Tanzania), and Lake Hirakud (India).

4. Discussion

The unique datasets from the Lakes_cci and Fire_cci projects, providing global long-term consistent data at high temporal resolution, allowed us to develop one of the first studies into how the water quality of lakes responds to fire impacts via the terrestrial pathway at a global scale. The use of the SPR approach allowed for the identification of lakes that were potentially more prone to be affected in their water quality by fire-derived substances (burned materials and released nutrients) transported via terrestrial pathways in their catchments.

We investigated the effects of wildfires on lake water quality using different data analysis approaches to identify parameters that could help in explaining lake responses in terms of Chl-a and turbidity variations. These included the calculation of lake Chl-a and turbidity concentrations and peaks during the study period (2017–2020), as well as calculation of successive peaks in Chl-a and turbidity that developed after a fire occurred

in a lake catchment. In addition, with the purpose of detecting fire-induced short-term changes in lake water quality, we compared pre- and post-fire values of Chl-a and turbidity within six months after a major fire occurrence in their catchment. Time series plots of indicative parameters for fires, catchments, weather (SPI), and lake water quality responses were also generated, with graphical analysis used to investigate the temporal succession of events in the catchment of the selected lakes and to support global findings.

Among the large number of hydro-morphological lake characteristics considered in the analysis, we found that lake average depth was a significant factor for determining the Chl-a concentration of maximum peaks, as values differentiated among three lake depth typologies (shallow, medium, and deep), being typically higher in shallower lakes. This result was confirmed by multiple linear regression, since lake depth was a significant negative parameter for predicting maximum Chl-a peaks concentration, followed by lake latitude (+), mean ratio BA/A (+), which is a proxy for the extension of the fire event, and mean SPI (−). The results of our study, finding higher Chl-a in shallower lakes than in deeper lakes, are in agreement with other studies [56,57] concluding that water transparency and Chl-a concentration in European lakes were greatly related to lake depth, with shallow lakes having higher Chl-a and deep lakes having higher transparency. Shallow lakes typically have higher production per unit area when compared to deep lakes with similar phosphorus and total dissolved matter concentrations, as a result of faster nutrient cycling and better mixing and lighting conditions [58,59]. For fire-burned materials and soil-released nutrients transported via a terrestrial pathway, especially by increased runoff in a lake catchment after precipitation events, the morphology of the final receptor lake is therefore a determinant for the internal process dynamics and ultimately for lake primary production [8]. It is long acknowledged that lake basin morphology plays a key role in modulating lake water quality, and in particular depth has important consequences on mixing regimes, light, and nutrient availability, affecting biological production and processes within a lake. Early studies on lake eutrophication such as that by Vollenweider [60] developed empirical relationships between lake mean depth and tolerable phosphorous loading, with mean depth also important in representing a general indicator of hydraulic residence time [61]. The inclusion of latitude as a positive influence on the Chl-a maximum peak was surprising as the higher temperatures in the tropics lead to more efficient nutrient cycling and higher primary production [62]; however, concentrations of phosphorous and nitrogen have been reported as around double that of the tropics at mid-temperate regions and this may explain the positive relationship [63]. In addition, in broader terms, other secondary impacts of relevance for lake ecosystems include the reduction in oxygen concentrations which can result not only from an increase in chlorophyll-a levels but are also regulated by dissolved organic matter and lake area [64,65].

In general, we found weak global relationships between burned areas in catchments and lake Chl-a or turbidity concentrations in our study. Finding strong relationships also proved to be difficult in other studies of wildfire impacts on freshwater systems [5], as findings suggested that the percentage of area burned did not affect the extent to which nutrient concentrations would increase after a fire. In a recent study of 15 lakes in the Superior National Forest in Minnesota [28], no post-wildfire changes were found in Chl-a despite significant increases in total phosphorous and total nitrogen in lakes with burned watersheds. However, in our SMLR analysis, we found that the inclusion of the mean ratio of burned area/burnable area as a secondary factor potentially represented an indication of fire impact on Chl-a peaks (+), likely induced by the input of nutrients to lakes released after a fire. Within a restricted group of lakes affected by important and regular fires, located in Africa, again depth was the most significant factor influencing Chl-a peaks and the burned area closer to the lake (calculated as level 0–4 in our study) was a secondary, although negative (−), weak factor. In this restricted lake group, the water residence time (+) was also a significant positive factor in determining Chl-a maximum peaks. A higher water residence time is generally related to greater primary production, with a longer time available for phytoplankton to utilize nutrients, and the persistence and the entirety of

fire effects on lake ecosystems may increase with water residence time [3], with potential consequences on Chl-a increases.

The results for lake turbidity responses to fires indicated a potential dependence on lake catchment and local weather conditions, with the precipitation index (SPI) in the SMLR analysis as a significant primary but weak factor for predicting turbidity maximum peak development. Within the restricted group of African lakes, additional catchment characteristics such as lake elevation (−) and the ratio catchment area/lake area (+) were significant. For turbidity, the location and the size of the lake catchment and how efficiently burned materials produced by wildfires are transported to a lake are key factors, since increases in turbidity concentration (especially when detected by satellite images) might be related to the load of burned material and sediments to a lake. River sediment yield has been estimated to increase with increases in area burned [66]. The ratio catchment area/lake area was also important for lake turbidity conditions and responses since lakes with larger ratios catchments/lake area tend to be more affected by catchment characteristics and dynamics, with stronger influences on their water chemistry. These lakes would be also more prone to the effects of wildfires, since post-fire hydrological processes in their drainage area, such as increased runoff and transport of burned material via terrestrial pathways, will be more effective in determining lake turbidity conditions and variations. In our dataset for instance, Lake Henrik (South Africa) has a large catchment area (70,460 km^2), a high ratio catchment area/lake area (239), and very turbid waters (annual mean of 35 NTU), developing major peaks of turbidity concentration (up to a maximum of 202 NTU). Although precipitation generally promoted an increase in lake turbidity, on the other hand direct precipitation on the lake surface might dilute terrestrial inputs, resulting in an overall decrease in turbidity concentration. Lathrop [67] found that larger lakes have a greater capability of diluting the inputs of transported material from burned areas, even when a significant proportion of the lake catchment area was burned (25%). When evaluating fire effects on global lakes via terrestrial pathways after precipitation events, the increased turbidity from post-fire runoff might thus be difficult to detect consistently, due to the concurrent diluting effect of precipitation, especially for lakes of large surface area.

The impact that wildfires have on soil properties is intricate and depends on soil characteristics, fire intensity, and duration [68], with soil type and texture having an important role in influencing erosion [69]. A previous study found erodibility was a more important factor than hydrological changes in particulate export from a deforested catchment where regrowth was prevented but the influence of erodibility was only clearly visible after two years, complicating the timescale over which the full range of impacts may be expected [23]. In this study, soil type data were not available at global scale and could not be included in our analysis, thus limiting the interpretation of our findings for water quality responses.

Our study gave an indication of the timing of Chl-a and turbidity peaks occurring after a fire: the first detected turbidity peak and maximum Chl-a peak can highlight a succession of events in a lake catchment generated by terrestrial transport of burned materials and possibly of nutrients to the lake, inducing phytoplankton responses detected as Chl-a concentration changes. We found that lakes with a ratio BA/A > 0.25 and a burned area closer to the lake basin (level 0–4) tended to show a faster response to fire in developing a maximum Chl-a peak (90 days), suggesting a promoted and accelerated primary production by nutrient input to the lakes, possibly derived from the release of burned and eroded soils after fire occurrence. The peak timing in our results agree with Raoelison et al. [5], since nutrient concentration increase after a fire was generally significant within a year.

In our study, when considering global responses to fire occurrence in the less productive lakes (mean Chl-a < 5 mg m^{-3}), they were seen to respond slightly faster in terms of the timing of Chl-a development (days) after a fire, but with lower peaks in concentration than lakes at higher trophic conditions. A faster response in oligotrophic lakes might be related to their natural condition of nutrients limitation, with potential input from fire-induced runoff stimulating prompt phytoplankton growth. Although the maximum Chl-a concen-

tration reached was found to be proportional to lake trophic status (Figure 8b), it should be remembered that a relatively small increase in Chl-a concentration in a low productivity lake could be very ecologically relevant, promoting changes in the nature of the whole ecosystem. Some reasons for observing weaker Chl-a increments in oligotrophic lakes after a fire might be due to light reduction caused by fire-derived burned materials, as these lakes generally have high transparency (excluding humic lakes). These may be related to short-term reductions in light availability, which could inhibit phytoplankton growth during the first vegetative period after a fire, regardless of increased nutrient inputs [70,71], and oligotrophic clear lakes might be more sensitive to light attenuation caused by burned materials and increased dissolved organic carbon from runoff [26] than already less transparent and more turbid eutrophic lakes. Our findings align with recent studies [28] in shallow oligo-mesotrophic lakes, suggesting that clear unproductive lakes could experience post-fire increases in primary productivity, but also that post-fire dynamics of nutrients and light limitation are important factors. Results from studies on ecological assessments of European lakes [56] suggested that light conditions and mineral availability are significant drivers of Chl-a concentrations in oligotrophic lakes.

In our dataset, although the effects of wildfires on eutrophic lakes seemed to be translated into relatively higher Chl-a peaks, it is however difficult to partition the influence of fires from other sources, given their often very dynamic phytoplankton communities. Post-fire Chl-a increases associated with high rainfall may be derived as much or more from other catchment point and non-point sources as from wildfires.

Regarding land cover vegetation, we found differences among clusters of burned vegetation types in relation to Chl-a development timing after a fire, suggesting that vegetation communities might be an important factor in mediating responses in water ecosystems. However, precipitation events have likely played a concurrent role, as the highest maximum SPI was found for the vegetation cluster (Cluster 4—evergreen boreal forests) which had the fastest responses of Chl-a in lakes. Moreover, lakes included in the different clusters were located in diverse geographic areas (see map in Figure 1), with coniferous forests in Canada and North America (Cluster 4) and mixed deciduous broadleaves in the southern hemisphere (Cluster 6), indicating that biomes and their climatic variables, including related precipitation patterns, would be key factors for the temporal response of Chl-a.

Our last analysis aimed at comparing pre- and post-fire water quality conditions in our studied lakes. During a six-month period after a major fire, lake Chl-a either increased or decreased in a similar number of lakes, indicating that lake specific ecological context is important to explain and predict potential responses to fires. In other studies investigating the effects of wildfires on lakes, post-fire changes in lake concentrations (i.e., nutrients) were not regularly observed. De Palma-Dow et al. [27] did not find a substantial change in total phosphorous concentrations up to three years post-fire and found no changes in relation to smaller fires when analyzing Clear Lake (California), despite the very large burned area and its proximity to the lake (40% of the watershed burned at 1 km from the shoreline). A study of boreal Alaskan lakes [24] found that nutrient concentrations were not sensitive to wildfires up to two years after the event.

As climate change is a major contributor to significant wildfire events, floods, and extreme droughts, the effect on lake water quality conditions is in many ways unpredictable [72]. We analyzed in detail responses to fire occurrence in two African lakes with the largest burned areas recorded in this study and having different lake morphologies, the deep Lake Volta and the shallow and very large Lake Chad. In the former, lake Chl-a and turbidity concentrations remained stable with modest peak development, while in the latter more pronounced fluctuations were observed. Although Lake Volta had a greater ratio BA/A than Lake Chad, the response to wildfires was not accordingly more pronounced, likely due to lake morphology. Wildfire effects on lakes can be indeed highly site-specific, regardless of similarities in the geographical, morphological, and fire characteristics of lakes. In our study, for instance, we compared two African lakes in Zambia (Lake Mweru) and in

Congo (Lake Mukenge) sharing very similar morphological and ecological characteristics and also affected by comparable fires. While responses for turbidity were similar in the two lakes, patterns in Chl-a were different, with Lake Mweru showing greater and faster responses and with an overall increase in Chl-a six months after the major fire occurrence (+16%) while Lake Mukenge had a Chl-a decrease (−22%).

We observed that on occasion turbid conditions in lakes did not lead necessarily to successive Chl-a increases. Although lake turbidity might increase after wildfires as a result of increasing runoff and transport of burned material to the lake, this will not necessarily correspond to a related input of nutrients, as the majority of materials (debris, ashes, suspended material) will not be suitable for direct use by phytoplankton. Moreover, the increased water turbidity could reduce light availability for phytoplankton growth, resulting in an overall Chl-a decrease, as observed in our study for different lake typologies. Other studies investigating the effects of wildfires on lakes reported significantly reduced lake water transparency primarily due to increases in dissolved organic carbon [26,28] and in turbidity. Subsequent changes in primary productivity would be mediated by both light availability and nutrient conditions, making the ultimate response of lake water quality to wildfires unpredictable.

We have also to acknowledge that hydro-morphological features should be integrated to consider soil properties, such as type, moisture, and texture, as they have been shown to be important in determining the hydrological responses of landscapes following wildfires [73]. However, as our study had a more ecological rather than a hydrological modelling approach, the lack of inclusion of soil properties was considered less crucial.

5. Conclusions

This study intended to contribute to the global study of the effects of wildfires on lake water quality, including a large number of lakes in many regions worldwide and covering different lake types and ecological settings. To this aim, the satellite derived Lakes_cci and Fire_cci datasets were used and the SPR approach was applied to identify lakes most influenced by their catchment and likely to be more impacted by wildfires via a terrestrial pathway. Satellite derived Chl-a and turbidity variables were considered as indicators of changes in water quality induced by wildfires. The lakes affected by the biggest wildfires, in terms of burned areas extension, were located in the African continent and were characterized by regular annual fires. Lake morphology was important in determining lake responses, as among a large number of hydro-morphological lake characteristics, lake depth was found to be significant in determining Chl-a concentration peaks, with higher peaks in shallower than in deeper lakes. The standardized precipitation index was a candidate parameter for determining maximum turbidity peaks, with the probability of developing higher peaks in wetter conditions.

When analyzing globally the entire set of lakes, it was a challenging task to identify significant relationships between fires and lake water responses in terms of Chl-a and turbidity changes. When focusing on a restricted group of lakes (regular burning, in the African region) we found more significant relationships; therefore, partitioning lakes by location and wildfire frequency and intensity may aid in the understanding of relationships that are distinct globally. We finally found that during a six-month period after a major fire, lake Chl-a and turbidity either increased or decreased in a similar number of lakes, suggesting that lake specific ecological and hydro-morphological context is important to interpret potential responses to fires. Our findings are in agreement with previous local studies on the effect of fires on lakes, since comparison of pre- and post-fire lake water quality variables detected either changes or stability in lake conditions.

Defining lake responses to fires at global scale and generalizing findings proved to be difficult because of the many interactions among the variables involved, resulting in complex hydrological and ecological dynamics in lakes, eventually translated into water quality condition changes. Moreover, lake biological responses to fires are extremely complex and inconsistent among relevant studies, likely because organisms respond to

opposing factors that can simultaneously enhance or inhibit primary productivity. Nutrients flushing from soils in burned areas through runoff have the potential to promote primary production in a lake, while a reduction in light availability by increased turbidity can reduce phytoplankton growth.

Ideally, future studies should incorporate information on seasonal nutrient dynamics over a long timeframe so that loads derived from wildfires and other sources can be partitioned and related with greater confidence to in-lake responses in Chl-a and turbidity. Moreover, future works should combine remote sensing data with hydrological modelling to better quantify the role of precipitation, soil type, and runoff in explaining water quality changes due to fire effects. There exists an opportunity to pair with local authorities and practitioners to help further understand relationships. The incidence and intensity of wildfires is increasing globally, which together with increasing pressure on water quantity and quality in lakes is threatening many global communities who depend on them. This study underlines that the responses within lakes are dependent on factors such as lake depth and trophic conditions, as well as the timing and magnitude of the drought–fire–precipitation cycle. In many cases, however, no clear response was identified, indicating that some lakes may be resilient, probably depending on specific catchment properties and in-stream or in-lake processes. Although satellite remote sensing remains the most feasible approach for global analysis, delivering data at the required frequency and spatial scales needed, it might provide better ecological insights when combined with datasets from different sources.

Supplementary Materials: The following supporting information can be downloaded at https://www.mdpi.com/article/10.3390/app14062626/s1, Table S1. Indicator values for cluster analysis carried out on 2011 burned vegetation types (100% = perfect indicator i.e., Land Cover (LC) burn occurs in only that cluster); Table S2. List of 106 selected lakes (list and maps at this link: https://gws-access.jasmin.ac.uk/public/cds_c3s_lakes/CCI_LAKES/CCI_LAKE_LIST_v2/LAKE_LIST_MASK_CCI_v2_UoR_fv1.0.html accessed on 1 March 2022); Table S3. Results of the multinomial logistic regression analysis between category changes (increase, decrease) in chlorophyll-a (Chl-a) or turbidity and geographical factors, land cover, fire extension, and rainfall; Figure S1. Graphs of the percentage of the 106 lakes in each class of the following lake characteristics: mean chlorophyll-a (Chl-a) concentration for the period 2017–2020 (A), mean turbidity concentration for the period 2017–2020 (B), lake area (C), lake total volume (D), residence time (E), elevation (F); Figure S2. Result graphs of the boosted regression analysis to investigate the drivers of timing of first and maximum peaks of chlorophyll-a (Chl-a; upper graphs) and turbidity (lower graphs) after a fire occurrence.

Author Contributions: R.C.: Conceptualization, Methodology, Validation, Formal analysis, Writing Original Draft, Review and Editing. M.P.: Conceptualization, Methodology, Formal analysis, Writing—Original Draft, Review and Editing. G.F.: Conceptualization, Methodology, Writing—Review and Editing. D.S.: Methodology, Writing—Review and Editing. L.P.: Methodology, Formal Analysis. G.T.: Methodology, Formal Analysis. M.B.: Conceptualization, Methodology, Resources, Writing—Review and Editing. C.A.: Resources, Writing—Review and Editing. C.G.: Conceptualization and Design, Resources, Writing—Review and Editing. All authors have read and agreed to the published version of the manuscript.

Funding: This work is supported by the Lakes_cci (contract n. 40000125030/18/I-NB) and Fire_cci (contract n. 4000126706/19/I-NB) projects which are both part of the ESA Climate Change Initiative.

Institutional Review Board Statement: Not applicable.

Informed Consent Statement: Not applicable.

Data Availability Statement: Satellite products from both the Fire_cci and Lakes_cci projects were downloaded from the Centre for Environmental Data Analysis (CEDA, https://catalogue.ceda.ac.uk/, accessed on 14 September 2023) archive within the ESA_cci Open Data Portal project framework. Lake and catchment area data were downloaded from the global HydroSHEDS database (https://www.hydrosheds.org/page/hydrolakes, https://www.hydrosheds.org/products/hydrobasins accessed on 1 February 2022). The ERA5 reanalysis data were downloaded from Climata Data

Store (https://cds.climate.copernicus.eu/cdsapp#!/dataset/reanalysis-era5-single-levels?tab=form accessed on 1 January 2022).

Acknowledgments: We would like to thank Stefan Simis and Jean-François Crétaux for the useful discussion for the analysis developed in this study. We thank the three anonymous reviewers for their insightful and helpful comments in the development of this manuscript.

Conflicts of Interest: The authors declare no conflicts of interest.

References

1. Brown, K.P.; Gerber, A.; Bedulina, D.; Timofeyev, M.A. Human impact and ecosystemic health at Lake Baikal. *WIREs Water* **2021**, *8*, 1528. [CrossRef]
2. Woolway, R.I.; Jennings, E.; Shatwell, T.; Golub, M.; Pierson, D.C.; Maberly, S.C. Lake heatwaves under climate change. *Nature* **2021**, *589*, 402–407. [CrossRef]
3. McCullough, I.M.; Cheruvelil, K.S.; Lapierre, J.-F.; Lottig, N.R.; Moritz, M.A.; Stachelek, J.; Soranno, P.A. Do Lakes Feel the Burn? Ecological Consequences of Increasing Exposure of Lakes to Fire in the Continental United States. *Glob. Chang. Biol.* **2019**, *25*, 2841–2854. [CrossRef]
4. Liu, D.; Zhou, C.; Keesing, J.K.; Serrano, O.; Werner, A.; Fang, Y.; Chen, Y.; Masque, P.; Kinloch, J.; Sadekov, A.; et al. Wildfires Enhance Phytoplankton Production in Tropical Oceans. *Nat. Commun.* **2022**, *13*, 1348. [CrossRef] [PubMed]
5. Raoelison, O.D.; Valenca, R.; Lee, A.; Karim, S.; Webster, J.P.; Poulin, B.A.; Mohanty, S.K. Wildfire Impacts on Surface Water Quality Parameters: Cause of Data Variability and Reporting Needs. *Environ. Pollut.* **2023**, *317*, 120713. [CrossRef] [PubMed]
6. Bixby, R.J.; Cooper, S.D.; Gresswell, R.E.; Brown, L.E.; Dahm, C.N.; Dwire, K.A. Fire Effects on Aquatic Ecosystems: An Assessment of the Current State of the Science. *Freshw. Sci.* **2015**, *34*, 1340–1350. [CrossRef]
7. Williamson, C.E.; Overholt, E.P.; Brentrup, J.A.; Pilla, R.M.; Leach, T.H.; Schladow, S.G.; Warren, J.D.; Urmy, S.S.; Sadro, S.; Chandra, S.; et al. Sentinel Responses to Droughts, Wildfires, and Floods: Effects of UV Radiation on Lakes and Their Ecosystem Services. *Front. Ecol. Environ.* **2016**, *14*, 102–109. [CrossRef]
8. Pinardi, M.; Stroppiana, D.; Caroni, R.; Parigi, L.; Tellina, G.; Free, G.; Giardino, C.; Albergel, C.; Bresciani, M. Assessing the Impact of Wildfires on Water Quality Using Satellite Remote Sensing: The Lake Baikal Case Study. *Front. Remote Sens.* **2023**, *4*, 1107275. [CrossRef]
9. Holdgate, M.W. *A Perspective of Environmental Pollution*; Cambridge University Press: Cambridge, UK, 1979.
10. Sneddon, J. Source-Pathway-Receptor Investigation of the Fate of Trace Elements Derived from Shotgun Pellets Discharged in Terrestrial Ecosystems Managed for Game Shooting. *Environ. Pollut.* **2009**, *157*, 2663–2669. [CrossRef] [PubMed]
11. Environment Agency. *Guidance on Assessment of Risks from Landfill Sites—External Consultation Report*; Environment Agency: Bristol, UK, 2004.
12. Scottish Government. *Strategic Environmental Assessment (SEA) of Draft Plan for Offshore Wind Energy in Scottish Territorial Waters*; Scottish Government: Edinburgh, UK, 2010; Volume 1.
13. Narayan, S.; Hanson, S.; Nicholls, R.J.; Clarke, D.; Willems, P.; Ntegeka, V.; Monbaliu, J. A Holistic Model for Coastal Flooding Using System Diagrams and TheSource-Pathway-Receptor (SPR) Concept. *Nat. Hazards Earth Syst. Sci.* **2012**, *12*, 1431–1439. [CrossRef]
14. Horrillo-Caraballo, J.M.; Reeve, D.E.; Simmonds, D.; Pan, S.; Fox, A.; Thompson, R.; Hoggart, S.; Kwan, S.S.H.; Greaves, D. Application of a Source-Pathway-Receptorconsequence (SPRC) Methodology to the Teign Estuary. *UK J. Coast. Res.* **2013**, *65*, 1939–1944. [CrossRef]
15. Sun, D.; Wang, H.; Huang, J.; Zhang, J.; Liu, G. Urban Road Waterlogging Risk Assessment Based on the Source–Pathway–Receptor Concept in Shenzhen, China. *J. Flood Risk Manag.* **2023**, *16*, 12873. [CrossRef]
16. Shakesby, R.A.; Doerr, S.H. Wildfire as a Hydrological and Geomorphological Agent. *Earth-Sci. Rev.* **2006**, *74*, 269–307. [CrossRef]
17. Smith, H.G.; Sheridan, G.J.; Lane, P.N.J.; Nyman, P.; Haydon, S. Wildfire Effects on Water Quality in Forest Catchments: A Review with Implications for Water Supply. *J. Hydrol.* **2011**, *396*, 170–192. [CrossRef]
18. Robichaud, P.R.; Elliot, W.J.; Pierson, F.B.; Hall, D.E.; Moffet, C.A. Predicting Postfire Erosion and Mitigation Effectiveness with a Web-Based Probabilistic Erosion Model. *Catena* **2007**, *71*, 229–241. [CrossRef]
19. Malmon, D.V.; Reneau, S.L.; Katzman, D.; Lavine, A.; Lyman, J. Suspended Sediment Transport in an Ephemeral Stream Following Wildfire. *J. Geophys. Res. Earth Surf.* **2007**, *112*, F02006. [CrossRef]
20. Cannon, S.H.; Gartner, J.E.; Wilson, R.C.; Bowers, J.C.; Laber, J.L. Storm Rainfall Conditions for Floods and Debris Flows from Recently Burned Areas in Southwestern Colorado and Southern California. *Geomorphology* **2008**, *96*, 250–269. [CrossRef]
21. Moody, J.A.; Martin, D.A. Synthesis of Sediment Yields after Wildland Fire in Different Rainfall Regimes in the Western United States. *Int. J. Wildland Fire* **2009**, *18*, 96–115. [CrossRef]
22. Ebel, B.A.; Moody, J.A.; Martin, D.A. Hydrologic Conditions Controlling Runoff Generation Immediately after Wildfire. *Water Resour. Res.* **2012**, *48*, W03529. [CrossRef]
23. Bormann, F.H.; Likens, G.; Siccama, T.; Pierce, R.; Eaton, J. The Export of Nutrients and Recovery of Stable Conditions Following Deforestation at Hubbard Brook. *Ecol. Monogr.* **1974**, *44*, 255–277. [CrossRef]

24. Lewis, T.L.; Lindberg, M.S.; Schmutz, J.A.; Bertram, M.R. Multi-Trophic Resilience of Boreal Lake Ecosystems to Forest Fires. *Ecology* **2014**, *95*, 1253–1263. [CrossRef]
25. Carignan, R.; D'Arcy, P.; Lamontagne, S. Comparative Impacts of Fire and Forest Harvesting on Water Quality in Boreal Shield Lakes. *Can. J. Fish. Aquat. Sci.* **2000**, *57*, 105–117. [CrossRef]
26. McEachern, P.; Prepas, E.E.; Gibson, J.J.; Dinsmore, W.P. Forest Fire Induced Impacts on Phosphorus, Nitrogen, and Chlorophyll a Concentrations in Boreal Subarctic Lakes of Northern Alberta. *Can. J. Fish. Aquat. Sci.* **2000**, *57*, 73–81. [CrossRef]
27. De Palma-Dow, A.; McCullough, I.M.; Brentrup, J.A. Turning up the Heat: Long-term Water Quality Responses to Wildfires and Climate Change in a Hypereutrophic Lake. *Ecosphere* **2022**, *13*, e4271. [CrossRef]
28. McCullough, I.M.; Brentrup, J.A.; Wagner, T.; Lapierre, J.; Henneck, J.; Paul, A.M.; Belair, M.; Moritz, M.A.; Filstrup, C.T. Fire Characteristics and Hydrologic Connectivity Influence Short-Term Responses of North Temperate Lakes to Wildfire. *Geophys. Res. Lett.* **2023**, *50*, 103953. [CrossRef]
29. Zhao, Q.; Yu, L.; Du, Z.; Peng, D.; Hao, P.; Zhang, Y.; Gong, P. An Overview of the Applications of Earth Observation Satellite Data: Impacts and Future Trends. *Remote Sens.* **2022**, *14*, 1863. [CrossRef]
30. Plummer, S.; Lecomte, P.; Doherty, M. The ESA Climate Change Initiative (CCI): A European Contribution to the Generation of the Global Climate Observing System. *Remote Sens. Environ.* **2017**, *203*, 2–8. [CrossRef]
31. Lizundia-Loiola, J.; Otón, G.; Ramo, R.; Chuvieco, E. A Spatio-Temporal Active-Fire Clustering Approach for Global Burned Area Mapping at 250 m from MODIS Data. *Remote Sens. Environ.* **2020**, *236*, 111493. [CrossRef]
32. Carrea, L.; Crétaux, J.-F.; Liu, X.; Wu, Y.; Calmettes, B.; Duguay, C.R.; Merchant, C.J.; Selmes, N.; Simis, S.G.H.; Warren, M.; et al. Satellite-Derived Multivariate World-Wide Lake Physical Variable Timeseries for Climate Studies. *Sci. Data* **2023**, *10*, 30. [CrossRef]
33. Giglio, L.; Schroeder, W.; Justice, C.O. The Collection 6 MODIS Active Fire Detection Algorithm and Fire Products. *Remote Sens. Environ.* **2016**, *178*, 31–41. [CrossRef] [PubMed]
34. Defourny, P.; Lamarche, C.; Bontemps, S.; Maet, T.; Bogaert, E.; Moreau, I.; Brockmann, C.; Boettcher, M.; Kirches, G.; Wevers, J.; et al. *Land Cover Climate Change Initiative—Product User Guide v2*; ESA-UCLouvain-Geomatics: Louvain-la-Neuve, Belgium, 2017; Issue 2.0.
35. Baston, D.; ISciences, L.L.C. Exactextractr: Fast Extraction from Raster Datasets Using Polygons. R Package Version. 2022. Available online: https://CRAN.R-project.org/package=exactextractr.34 (accessed on 1 January 2022).
36. Messager, M.L.; Lehner, B.; Grill, G.; Nedeva, I.; Schmitt, O. Estimating the Volume and Age of Water Stored in Global Lakes Using a Geo-Statistical Approach. *Nat. Commun.* **2016**, *7*, 13603. [CrossRef] [PubMed]
37. Copernicus Climate Change Service Land Cover Classification Gridded Maps from 1992 to Present Derived from Satellite Observation. Copernicus Climate Change Service (C3S) Climate Data Store (CDS) 2019. Available online: https://cds.climate.copernicus.eu/portfolio/dataset/satellite-land-cover (accessed on 1 January 2022).
38. Edwards, D.C.; McKee, B.T. *Characteristics of 20th Century Drought in the United States at Multiple Time Scales*; Department of Atmospheric Science, Colorado State University: Fort Collins, CO, USA, 1997.
39. McCune, B.; Mefford, M.J. *Multivariate Analysis of Ecological Data. Version 7*; MjM Software Design: Gleneden Beach, OR, USA, 2016.
40. Free, G.; Bresciani, M.; Pinardi, M.; Simis, S.; Liu, X.; Albergel, C.; Giardino, C. Investigating Lake Chlorophyll-a Responses to the 2019 European Double Heatwave Using Satellite Remote Sensing. *Ecol. Indic.* **2022**, *142*, 109217. [CrossRef]
41. R Core Team. *R: A Language and Environment for Statistical Computing*; R Core Team: Vienna, Austria, 2019.
42. Zeileis, A.; Grothendieck, G. Zoo: S3 Infrastructure for Regular and Irregular Time Series. *J. Stat. Softw.* **2005**, *14*, 1–27. Available online: http://www.jstatsoft.org/v14/i06/ (accessed on 14 September 2023). [CrossRef]
43. Stockwell, J.D.; Doubek, J.P.; Adrian, R.; Anneville, O.; Carey, C.C.; Carvalho, L.; De Senerpont Domis, L.N.; Dur, G.; Frassl, M.A.; Grossart, H.-P.; et al. Storm Impacts on Phytoplankton Community Dynamics in Lakes. *Glob. Chang. Biol.* **2020**, *26*, 2756–2784. [CrossRef]
44. Council of the European Communities. Directive 2000/60/EC of the European Parliament and of the Council of 23 October 2000 Establishing a Framework for Community Action in the Field of Water Policy. *Off. J. Eur. Union* **2000**, *L327*, 72.
45. Moss, B.; Stephen, D.; Alvarez, C.; Becares, E.; Bund, W.V.; Collings, S.E.; Donk, E.V.; Eyto, E.D.; Feldmann, T.; Fernández-Aláez, C.; et al. The Determination of Ecological Status in Shallow Lakes—A Tested System (ECOFRAME) for Implementation of the European Water Framework Directive. *Aquat. Conserv. Mar. Freshw. Ecosyst.* **2003**, *13*, 507–549. [CrossRef]
46. Donis, D.; Mantzouki, E.; McGinnis, D.F.; Vachon, D.; Gallego, I.; Grossart, H.-P.; de Senerpont Domis, L.N.; Teurlincx, S.; Seelen, L.; Lürling, M.; et al. Stratification Strength and Light Climate Explain Variation in Chlorophyll a at the Continental Scale in a European Multilake Survey in a Heatwave Summer. *Limnol. Oceanogr.* **2021**, *66*, 4314–4333. [CrossRef]
47. Elith, J.; Leathwick, J.R.; Hastie, T. A Working Guide to Boosted Regression Trees. *J. Anim. Ecol.* **2008**, *77*, 802–813. [CrossRef] [PubMed]
48. Ridgeway, G.; Southworth, M.H.; RUnit, S. Package 'Gbm'. *Viitattu* **2013**, *10*, 40.
49. Wickham, H.; Romain, F.; Lionel, H.; Kirill, M. Dplyr: A Grammar of Data Manipulation; R Package Version; 2018. Available online: https://cran.r-project.org/web/packages/dplyr/index.html (accessed on 14 September 2023).
50. Ripley, B.; Venables, W.; Ripley, M.B. *Package 'Nnet'*; R Package Version; 2016; Volume 7, p. 700. Available online: https://cran.r-project.org/web/packages/nnet/ (accessed on 14 September 2023).

51. Wickham, H. Data Analysis. In *Ggplot2*; Elegant Graphics for Data Analysis; Springer International Publishing: Cham, Switzerland, 2016; pp. 189–201.
52. Kurz, I. Phosphorus Exports from Agricultural Grassland with Overland Flow and Drainage Water (Johnstown Castle). In *Quantification of Phosphorus Loss from Soil to Water, Final Report and Literature Review*; EPA: Wexford, Ireland, 2000; pp. 9–56.
53. Schindler, D.W. A Hypothesis to Explain Differences and Similarities Among Lakes in the Experimental Lakes Area, Northwestern Ontario. *J. Fish. Res. Board Can.* **1971**, *28*, 295–301. [CrossRef]
54. Engstrom, D.R. Influence of Vegetation and Hydrology on the Humus Budgets of Labrador Lakes. *Can. J. Fish. Aquat. Sci.* **1987**, *44*, 1306–1314. [CrossRef]
55. Rasmussen, J.B.; Godbout, L.; Schallenberg, M. The Humic Content of Lake Water and Its Relationship to Watershed and Lake Morphometry. *Limnol. Oceanogr.* **1989**, *34*, 1336–1343. [CrossRef]
56. Carvalho, L.; Solimini, A.; Phillips, G.; Berg, M.; Pietiläinen, O.-P.; Lyche Solheim, A.; Poikane, S.; Mischke, U. Chlorophyll Reference Conditions for European Lake Types Used for Intercalibration of Ecological Status. *Aquat. Ecol.* **2008**, *42*, 203–211. [CrossRef]
57. Nõges, T. Relationships between Morphometry, Geographic Location and Water Quality Parameters of European Lakes. *Hydrobiologia* **2009**, *633*, 33–43. [CrossRef]
58. Schindler, D.E.; Scheuerell, M.D. Habitat Coupling in Lake Ecosystems. *Oikos* **2002**, *98*, 177–189. [CrossRef]
59. Mehner, T.; Diekmann, M.; Brämick, U.; Lemcke, R. Composition of Fish Communities in German Lakes as Related to Lake Morphology, Trophic State, Shore Structure and Human-Use Intensity. *Freshw. Biol.* **2005**, *50*, 70–85. [CrossRef]
60. Vollenweider, R.A. *Scientific Fundamentals of the Eutrophication of Lakes and Flowing Waters, with Particular Reference to Nitrogen and Phosphorus as Factors in Eutrophication*; Organisation for Economic Co-operation and Development: Paris, France, 1968; Volume 192, p. 14.
61. Horne, A.J.; Goldman, C.R. *Limnology*, 2nd ed.; McGraw-Hill: New York, NY, USA, 1994.
62. Lewis, W.M., Jr. Tropical Lakes: How Latitude Makes a Difference. *Perspect. Trop. Limnol.* **1996**, *4364*, 43–64.
63. Abell, J.M.; Özkundakci, D.; Hamilton, D.P.; Jones, J.R. Latitudinal Variation in Nutrient Stoichiometry and Chlorophyll-Nutrient Relationships in Lakes: A Global Study. *Fundam. Appl. Limnol.* **2012**, *181*, 1–14. [CrossRef]
64. Crisman, T.L.; Chapman, L.J.; Chapman, C.A. Predictors of Seasonal Oxygen Levels in Small Florida Lakes: The Importance of Color. *Hydrobiologia* **1998**, *368*, 149–155. [CrossRef]
65. Søndergaard, M.; Jensen, J.P.; Jeppesen, E. Role of Sediment and Internal Loading of Phosphorus in Shallow Lakes. *Hydrobiologia* **2003**, *506*, 135–145. [CrossRef]
66. Grangeon, T.; Vandromme, R.; Cerdan, O.; Lo Porto, A. Modelling Forest Fire and Firebreak Scenarios in a Mediterranean Mountainous Catchment: Impacts on Sediment Loads. *J. Environ. Manag.* **2021**, *289*, 112497.
67. Lathrop, R. Impacts of the 1988 Wildfires on the Water-Quality of Yellowstone and Lewis Lakes, Wyoming. *Int. J. Wildland Fire* **1994**, *4*, 169–175. [CrossRef]
68. Agbeshie, A.A.; Abugre, S.; Atta-Darkwa, T.; Awuah, R. A Review of the Effects of Forest Fire on Soil Properties. *J. For. Res.* **2022**, *33*, 1419–1441. [CrossRef]
69. Noske, P.J.; Lane, P.N.; Nyman, P.; Van der Sant, R.E.; Sheridan, G.J. Predicting Post-wildfire Overland Flow Using Remotely Sensed Indicators of Forest Productivity. *Hydrol. Process.* **2022**, *36*, e14769. [CrossRef]
70. Allen, E.W.; Prepas, E.E.; Gabos, S.; Strachan, W.; Chen, W. Surface Water Chemistry of Burned and Undisturbed Watersheds on the Boreal Plain: An Ecoregion Approach. *J. Environ. Eng. Sci.* **2003**, *2*, 73–86. [CrossRef]
71. Ranalli, A.J. *A Summary of the Scientific Literature on the Effects of Fire on the Concentration of Nutrients in Surface Waters*; US Geological Survey: Reston, VA, USA, 2004.
72. Mishra, A.; Alnahit, A.; Campbell, B. Impact of Land Uses, Drought, Flood, Wildfire, and Cascading Events on Water Quality and Microbial Communities: A Review and Analysis. *J. Hydrol.* **2021**, *596*, 125707. [CrossRef]
73. Sheridan, G.J.; Nyman, P.; Langhans, C.; Cawson, J.; Noske, P.J.; Oono, A.; Van der Sant, R.; Lane, P.N. Is Aridity a High-Order Control on the Hydro–Geomorphic Response of Burned Landscapes? *Int. J. Wildland Fire* **2015**, *25*, 262–267. [CrossRef]